Only a subset of Met-activated pathways are required to sustain oncogene addiction

Only a Subset of Met-Activated Pathways Are Required to Sustain Oncogene Addiction

Andrea Bertotti[1], Mike F. Burbridge[2,*], Stefania Gastaldi[1,*], Francesco Galimi[1,*], Davide Torti[1,*], Enzo Medico[3], Silvia Giordano[1], Simona Corso[1], Gaëlle Rolland-Valognes[4], Brian P. Lockhart[4], John A. Hickman[2], Paolo M. Comoglio[1,†], and Livio Trusolino[1,†]

+Author Affiliations

[1]Division of Molecular Oncology, Institute for Cancer Research and Treatment (IRCC), University of Torino Medical School, 10060 Candiolo (Torino), Italy.

[2]Cancer Research and Drug Discovery, Institut de Recherches Servier, 78290 Croissy-sur-Seine, France.

[3]Laboratory of Functional Genomics, The Oncogenomics Center, Institute for Cancer Research and Treatment (IRCC), University of Torino Medical School, 10060 Candiolo (Torino), Italy.

[4]Division of Molecular Pharmacology and Pathophysiology, Institut de Recherches Servier, 78290 Croissy-sur-Seine, France.

[†]To whom correspondence should be addressed. E-mail: livio.trusolino@ircc.it (L.T.) and paolo.comoglio@ircc.it (P.M.C.)

* These authors contributed equally to this work.

ABSTRACT

Tumor onset and progression require the accumulation of many genetic and epigenetic lesions. In some cases, however, cancer cells rely on only one of these lesions to maintain their malignant properties, and this dependence results in tumor regression upon oncogene inactivation ("oncogene addiction"). Determining which nodes of the many networks operative in the transformed phenotype specifically mediate this response to oncogene neutralization is crucial to identifying the vulnerabilities of cancer. Using the Met receptor as the major model system, we combined multiplex phosphoproteomics, genome-wide expression profiling, and functional assays in various cancer cells addicted to oncogenic receptor tyrosine kinases. We found that Met blockade affected a limited subset of Met downstream signals: Little or no effect was observed for several pathways downstream of Met; instead, only a restricted and pathway-specific signature of transducers and transcriptional effectors downstream of Ras or phosphoinositide 3-kinase (PI3K) was inactivated. An analogous signature was also generated by inhibition of epidermal growth factor receptor in a different cellular context, suggesting a stereotyped response that likely is independent of receptor type or tissue origin. Biologically, Met inhibition led to cell-cycle arrest. Inhibition of Ras-dependent signals and PI3K-dependent signals also resulted in cell-cycle arrest, whereas cells in which Met was inhibited proliferated when Ras or PI3K signaling was active. These findings uncover "dominant" and "recessive" nodes among the numerous oncogenic networks regulated by receptor tyrosine kinases and active in cancer, with the Ras and PI3K pathways as determinants of therapeutic response.

INTRODUCTION

Because of the genomic instability inherent in cancer, neoplastic cells accrue genetic alterations and undergo genetic drift over time. Nevertheless, some tumors appear to be completely dependent on one single overactive oncogene for their growth and survival, so that when this oncogene is therapeutically inactivated, the cancer cells experience cell-cycle arrest, undergo apoptosis, or both. This reliance of some tumors on the activity of a single oncogene for continued cell proliferation and survival is described as "oncogene addiction," a phenomenon of unknown molecular mechanisms (*1*). Oncogene addiction may explain the clinical responses to cancer therapies targeting catalytically active oncogenic proteins, for example, cases of disease remission

in patients with chronic myelogenous leukemia treated with imatinib (an inhibitor of the tyrosine kinase ABL) and tumor shrinkage in patients with non–small cell lung carcinomas (NSCLCs) treated with gefitinib or erlotinib, both of which inactivate the epidermal growth factor receptor (EGFR), a receptor tyrosine kinase (*2*, *3*). All these responsive tumors exhibit a constitutively hyperactive form of the "druggable" molecule, which arises from genetic corruptions, such as point mutations, gene amplification, or chromosomal translocation (*2–4*).

Receptor tyrosine kinases represent attractive candidates for targeted therapies because their activity is often deregulated in cancer and because they can be inactivated by either monoclonal antibodies against receptor ectodomains or small-molecule inhibitors that block intracellular catalytic activity (*5*). Although much information is available about the transduction pathways that are called into action when basally inactive receptor tyrosine kinases are stimulated (*6*), less is known about the modulations in signaling pathways that occur when chronically hyperactive tyrosine kinases are inhibited. This latter scenario is more complex, because the long-term, deregulated activity of tyrosine kinase oncogenes is likely somewhat counteracted by reactive adaptation, including deterioration or desensitization of some signals and activation of compensatory pathways and of positive and negative feedback circuits (*1*, *7*, *8*).

We applied an integrated approach to identify the signaling and transcriptional perturbations produced by inhibition of the tyrosine kinase receptor Met, which is aberrantly activated in many human cancers as a result of gene amplification, transcriptional up-regulation, point mutations, or ligand [hepatocyte growth factor (HGF)] autocrine loops (*9*, *10*). Cell lines displaying amplification of the *MET* gene respond to Met inactivation with inhibition of proliferation, suggesting that this type of genetic aberration drives addiction to Met activity in vitro and may predict effective treatment outcome in vivo (*11*, *12*). In patients, *MET* amplification is associated with both de novo and acquired resistance to gefitinib in EGFR-mutant NSCLCs; pharmacologic inhibition of Met in EGFR-mutant, *MET*-amplified NSCLC cell lines restores sensitivity to gefitinib in vitro (*13–15*), highlighting the therapeutic potential of combination therapies against Met and EGFR in gefitinib-resistant tumors. All these findings have prompted the development of several antibodies that functionally block Met, as well as small-molecule Met inhibitors, many of which are in early-phase clinical trials (*10*, *16–18*). However, a systematic analysis of Met response effectors is lacking.

Using quantitative assessment of cell sensitivity to various single and combinatorial treatments, gene-oriented sequencing analysis, antibody-based phosphoproteomics, genome-wide expression profiling, and bioinformatics, we derived a biochemical and genetic blueprint that correlates with and is causally involved in the cell-cycle arrest provoked by Met inhibition in Met-addicted cancer cells. Unexpectedly, we found that cell-cycle arrest is not accompanied by a comprehensive rewiring of Met-dependent signaling networks; rather, Met inhibition selectively affects a limited compendium of signals and transcriptional effectors downstream of Ras and phosphoinositide 3-kinase (PI3K). Other transduction pathways that regulate Met-driven tumor growth in various settings, such as signals mediated by signal transducers and activators of transcription (STATs), the inhibitor of κBα (IκBα) and nuclear factor κB (NF-κB) (IκBα/NF-κB) pathway, c-Jun N-terminal kinase (JNK) signaling, and the p38 mitogen-activated protein kinase (MAPK) pathway, were unaltered or displayed minor changes after Met inhibition. This circumscribed Ras and PI3K "signature" may be a stereotyped response shared among different receptor tyrosine kinases, because it was substantially reproduced (although not completely phenocopied) by EGFR blockade in an EGFR-addicted cellular context. Moreover, the functional role of this signature appeared to be nonredundant: Pharmacologic inhibition of major signaling components along the Ras and PI3K axes was sufficient to recapitulate the proliferative block induced by Met inhibition, whereas genetic hyperactivation of the same components was sufficient to elude cell-cycle arrest. Together, these findings suggest that proliferation of cells addicted to tyrosine kinase oncogenes

depends on a restricted spectrum of intracellular mediators, which reveals a patent vulnerability of cancer and provides hints for future therapeutic approaches.

RESULTS

Met inhibition selectively modulates the activity of Ras- and PI3K-dependent signals

Proliferation of cell lines with amplification of the *MET* gene is severely impaired by pharmacologic or genetic inhibition of Met (*11*, *12*, *19*). We confirmed this finding using GTL16, a gastric carcinoma cell line that contains 11 extra copies of the *MET* locus (*20*). GTL16 cultured in 10% serum displayed considerable inhibition of proliferation when treated with the Met-specific inhibitor PHA-665752 (subsequently referred to as PHA) (*21*), but were completely insensitive to the EGFR inhibitor gefitinib (Fig. 1A). Cell proliferation was monitored with a "viability assay" of adenosine 5′-triphosphate (ATP) content, which is a proxy for cell number in situations where the cells are not dying. Fluorescence-activated cell sorting (FACS) analysis of propidium iodide–stained cells at 24, 48, and 72 hours after exposure to PHA revealed a progressive depletion of cells in the S phase along with an increase of cells in the G_0-G_1 phase. The fraction of cells belonging to the sub-G_1 population, which identifies apoptotic remnants, was low at all the time points examined, indicating that the major effect of this drug treatment is cell-cycle arrest (Fig. 1B). Furthermore, cell numbers remained constant upon prolonged (8 days) administration of PHA, and drug withdrawal after such an incubation period restored cell proliferation (Fig. 1C). Hence, upon deprival of Met signals, cells become quiescent but are not irreversibly committed to apoptosis.

To identify effectors involved in drug sensitivity, we analyzed the signaling consequences of Met blockade in GTL16 with antibody-based phosphoproteomics. We pursued a medium-scale strategy in which we investigated a panel of phosphoproteins modulated by Met activity and functionally involved in Met-driven proliferation and survival, including other receptor tyrosine kinases, Ras effectors [members of the extracellular signal–regulated kinase (ERK) cascade and PI3K-dependent signals], STATs, the IκBα–NF-κB complex, and MAPKs of the JNK and p38 family (*22*–*24*). All these signals are triggered by short-term treatment with HGF and are inhibited when this transient HGF stimulation is performed in the presence of a Met inhibitor (*22*). For most of the pathways, both intermediate transducers and downstream components were assayed, including phosphorylation-regulated transcription factors, for a total of 21 phosphoproteins analyzed (Fig. 1D). The amount of phosphorylated protein was assessed using analytical tools on the basis of antibodies specific for the phosphoproteins (table S1). To increase the number of antibodies available for analysis, we used two different technological platforms, Luminex and MesoScale (see Materials and Methods for details). Both technologies perform multiplex detection of changes in protein phosphorylation from individual lysates, allowing the acquisition of multiparametric information from relatively small cellular preparations. In addition, phosphoprotein variations are recorded numerically, which permits digital prioritization of signal activity, as well as interassay comparative reproducibility. Many antibodies were validated by exposing cells to stimuli that modulate the phosphorylation status of the protein of interest (fig. S1). A dose-response curve in GTL16 cells exposed for 2 hours to increasing concentrations of PHA in 10% serum revealed that Met autophosphorylation was completely inhibited at doses of 0.4 μM and higher (Fig. 1E). Hence, this incubation period (2 hours) and this inhibitor concentration (0.4 μM) were used for phosphoproteomic analysis. For control purposes we used 0.4 μM gefitinib, a dose sufficient to abrogate EGFR autophosphorylation and to inhibit proliferation in EGFR-addicted colon carcinoma cells (DiFi).

Phosphoproteomic analysis revealed a discernible pattern of signal modification upon Met blockade (the "biochemical response signature") (Fig. 1F; for numerical data, see table S1). PHA,

but not gefitinib, inhibited phosphorylation of the EGFR family members EGFR and ErbB2 (Fig. 1F and table S1), which is consistent with previous studies (*25*) and indicates that amplified *MET* lies at the apex of a signaling hierarchy in which other tyrosine kinase receptors are passively transphosphorylated by the dominant oncogenic protein.

Among the many downstream signals explored, we detected a specific and pathway-oriented extinction in the phosphorylation of proximal and distal transducers of the Ras pathway. The major targets of Ras activity comprise two parallel and partly overlapping signaling arms, the RAF-MEK-ERK cascade and the PI3K-AKT axis; tyrosine kinases can also activate PI3K-AKT signals in a Ras-independent manner (Fig. 1D). The ERK cascade appeared to be globally inhibited, including MEK1 and 2 (MEK1/2), ERK1 and 2 (ERK1/2), the ERK substrate p90 ribosomal S6 kinase (p90RSK), and c-JUN. AKT phosphorylation was also decreased, as was the serine-threonine phosphorylation of molecules downstream of AKT, such as glycogen synthase kinase–3β (GSK-3β), the mammalian target of rapamycin (mTOR) effector p70 ribosomal S6 kinase (p70S6K), and phosphorylation of insulin receptor substrate 1 (IRS1) at the site phosphorylated by p70S6K (Fig. 1F and table S1). In contrast, other pathways that are stimulated by Met activation exhibited scant changes in response to Met inhibition or, in some cases, were unaffected (Fig. 1F and table S1): Such "indifferent" molecules included those that participate in Met-triggered invasive growth (STAT2 and 3 and components of the IκBα–NF-κB system), those that mediate transformation by oncogenic Met (JNK), and those that stimulate Met-dependent proliferation [the p38 MAPK effectors activating transcription factor 2 (ATF2) and heat shock protein 27 (HSP27)] (*26*–*32*). Met inhibition did not substantially alter the phosphorylation state of other MAPK-regulated molecules distal to the receptor, including cAMP (adenosine 3′,5′-monophosphate) response element–binding protein (CREB) and retinoblastoma (Rb) (Fig. 1F and table S1).

The multiparametric results were confirmed by enzyme-linked immunosorbent assays (ELISAs) or Western blotting with phosphorylation-specific antibodies. After a 2-hour treatment with 0.4 μM PHA, we observed only a partial reduction in the phosphorylation of STAT3 and JNK and no changes in the phosphorylation of NF-κB and p38 MAPK (fig. S2). Conversely, increasing concentrations of PHA progressively reduced and ultimately eliminated the phosphorylated (and activated) forms of ERK1/2 and AKT (fig. S3A); complete inhibition of phosphorylation of both ERK1/2 and AKT was readily achieved within 30 min after PHA treatment (1 μM) and persisted as long as 48 hours (fig. S3B). Finally, to validate the results obtained with PHA, we halted Met activation with an inducible system of RNA interference (RNAi) (*19*). Doxycycline-regulated activation of Met-targeted RNAi led to a quantitative decrease in abundance of Met and strong reduction of ERK1/2 and AKT phosphorylation (fig. S3C). On the basis of phosphoproteomic analysis, many of the transducers dephosphorylated by PHA treatment appeared to be also affected by Met genetic knockdown (fig. S3D).

Met inhibition generates a transcriptional signature that includes genes encoding proteins in the Ras and PI3K pathways

Our phosphoproteomic analysis was a knowledge-driven approach that relied on the availability of phosphoprotein-specific antibodies and implicated a preliminary selection of the measured parameters. We expanded the analysis with an unbiased, large-scale strategy of global pathway interrogation that involves DNA microarrays followed by ad hoc computational tools.

GTL16 cells were maintained in complete medium supplemented with 10% serum in the presence or absence of 1 μM PHA or 1 μM gefitinib for 24 hours. In concordance with the phosphoproteomic data, treatment with gefitinib did not induce any significant variation in the expression profile of GTL16 cells (24,000 genes explored) (Fig. 2A). In contrast, a total of 581 transcripts (267 up-regulated and 314 down-regulated) displayed a significant variation (fold change >2 and $P < 0.001$) after treatment with PHA. We call this set of 581 transcripts the "transcriptional response signature"

(Fig. 2A and table S2). We also compared the transcriptional response signature generated by Met pharmacologic inhibition with gene expression changes produced by doxycycline-regulated, RNAi-mediated knockdown of Met. Qualitatively, 98% of the transcripts significantly modulated by PHA treatment (572 of 581) were retrieved as statistically significant also in response to Met genetic ablation (fig. S3, E and F). Quantitatively, the extent of the expression changes was, on average, higher after Met knockdown than after Met catalytic inactivation (fig. S3E). PHA (1 μM) did not affect the gene expression profiles of colon carcinoma cells (DiFi), featuring *EGFR* amplification and a normal *MET* gene copy number (table S2). Hence, the PHA-mediated transcriptional response signature is robust and specific.

In an initial classification of the modulated genes, we used the David bioinformatic platform (*33*) for Gene Ontology (GO) annotations. Almost half of the regulated genes appeared to be associated with metabolic processes: Many of the transcripts depressed by Met inhibition fell into the categories of translation, amino acid synthesis, and transport, whereas several positively regulated genes pertained to functions related to chromatin remodeling and lipid metabolism (functional categories and their enrichment in regulated genes are reported in table S3). This suggests that Met blockade in Met-addicted cells causes a state of inertia that globally affects the cell's homeostatic machinery, with generalized reduction of protein synthesis and induction of chromatin condensation.

Smaller sets of genes were related to cell cycle and proliferation (~14% of the modulated genes), stress responses (10%), and cell death or apoptosis (8%) (table S3). Among such genes, many positive effectors of cell-cycle progression, such as cyclin-D1 (encoded by *CCND1*), c-MYC, and E2F family members, were suppressed by Met inhibition, whereas negative regulators of proliferation, for example, the cyclin-dependent kinase inhibitor p57Kip2 (encoded by *CDKN1C*) and the tumor suppressor caveolin-1 (encoded by *CAV1*), were induced (Fig. 2B). Altogether, these findings integrate well with the biological phenotype of Met-inhibited GTL16 and reinforce the notion that inactivation of the addictive oncogene leads to replication arrest.

To better characterize the signaling pathways regulating the changes observed in the expression profiles, we used the "gene set enrichment analysis" tool (GSEA). This approach considers gene sets (groups of genes related through a common function, pathway, or other property, according to published works) and tests whether the genes that are over- or underexpressed in each profiled tissue or cell line include a higher fraction of genes than randomly expected from a particular gene set (*34*). GSEA is a method for deriving the functional role of signaling networks from genome-wide expression data sets (*35*, *36*). With GSEA, we generated a list of gene sets either down- or up-regulated by Met inhibition (table S4). Among the gene sets significantly suppressed by PHA, there were signatures correlated with cell-cycle progression, including transcripts induced by c-MYC (called SCHUMACHER_MYC_UP) (*37*) or modulated by serum (called SERUM_FIBROBLAST_CORE_UP and SERUM_FIBROBLAST_CORE_DN) (*38*), and genes regulated by E2F1 (called REN_E2F1_TARGETS) (*39*) (FDR ≤0.001 for all four gene sets) (Table 1 and table S4). This is in accordance with the GO-supervised analysis and consistent with the proliferation block observed in response to Met inhibition, confirming the efficacy of GSEA in extracting functional information.

Intriguingly, GSEA reported two gene sets related to inhibition of Ras-dependent signals and PI3K-dependent signals, namely, signatures derived from K-RAS knockdown (K-RAS-KD; called CORDERO_KRAS_KD) (*40*) and rapamycin treatment (called PENG_RAPAMYCIN), which inhibits mTOR, an effector of PI3K signaling (*41*). In particular, the gene sets annotated as down-modulated by K-RAS-KD (CORDERO_KRAS_KD_VS_CONTROL_DN) or rapamycin (PENG_RAPAMYCIN_DN) appeared to be significantly suppressed by PHA (FDR <0.001 for

both); symmetrically, the transcripts up-regulated in response to K-RAS inactivation (CORDERO_KRAS_KD_VS_CONTROL_UP; FDR = 0.02) or rapamycin (PENG_RAPAMYCIN_UP; FDR = 0.012) were retrieved among the PHA-induced gene sets (Table 1and table S4). We validated the reproducibility and consistency of our gene expression profiling by TaqMan low-density quantitative polymerase chain reaction (qPCR) arrays on the six genes with the highest enrichment score for each of the eight gene sets listed in Table 1. According to this analysis, on the basis of two independent experiments, 41 of 48 transcripts (85%) showed strong positive correlation with the values for the same genes provided by microarray data (fig. S4). TaqMan validation was also extended to a panel of cell lines that includes additional *MET*-amplified, drug-sensitive cells (*11*, *12*, *42*), namely, other three gastric carcinoma cell lines (MKN45, SNU5, and HS746T) and one NSCLC cell line (EBC1). Overall, the results confirmed those obtained in GTL16: Positive correlation with microarray analysis was shown for 81% of the transcripts in MKN45, 87% in SNU5, 73% in HS746T, and 75% in EBC1 (table S5). This highlights a common profile of transcript modulation that correlates with *MET*amplification and, in large part, does not seem to depend on cell type or tissue origin.
The finding that treatment with PHA leads to an enrichment of gene sets altered by knockdown of Ras or by mTOR inhibition provides a genetic foundation for the involvement of signals downstream of Ras or PI3K in the cellular response to Met blockade and confirms the phosphoproteomic results. Notably, the signaling pathways almost or completely unaffected by Met inactivation (according to phosphoproteomic analysis) did not produce statistically significant genomic readouts providing further support for a role for Ras and PI3K pathways as selective transducers of sensitivity to Met inhibition.

Met and EGFR inhibition produce similar response signatures

To analyze whether this pathway-specific response is specific to Met-addicted cells or is a general characteristic of tumor cells that are addicted to receptor tyrosine kinases, we extended the phosphoprotein and gene expression profiling to cells endowed with hyperactive EGFR. We compared GTL16 (Met-addicted) and DiFi (EGFR-addicted). DiFi is a colon carcinoma cell line that features an amplification of the *EGFR* gene (*43*) and displays reciprocal analogies with Met-addicted cellular models: DiFi cells express a basally hyperactive EGFR (Fig. 3A), respond to gefitinib-mediated EGFR inhibition with a dose-dependent reduction of EGFR autophosphorylation (Fig. 3A) and a substantial growth arrest (Fig. 3B), and are completely insensitive to PHA (Fig. 3B).

Phosphoproteomic cross-analysis revealed that the pattern of phosphoprotein modulation is, in most cases, similar between the two cell lines (Fig. 3C and table S1). In analogy with PHA-treated GTL16, DiFi cells treated with 0.4 μM gefitinib for 2 hours displayed decreased phosphorylation of EGFR and other receptor tyrosine kinases, including Met, and moderate to strong reduction in the phosphorylation of signals dependent on Ras or PI3K, including MEK1/2, ERK1/2, p90RSK, AKT, GSK-3β, p70S6K, and IRS1. JNK, the p38 MAPK effectors ATF2 and HSP27, and the distal regulators CREB and Rb, were relatively unchanged, in accordance with the PHA-treated GTL16 cells. Phosphorylation of NF-κB was reduced; however, this occurred in both gefitinib-sensitive DiFi and gefitinib-insensitive GTL16, suggesting some nonspecific activity of the drug. Consistent with this interpretation, EGFR inhibition did not change the activation state of IκBα, the major NF-κB upstream regulator, further supporting an off-target effect. The only signaling molecule that appeared to be additionally down-modulated by EGFR blockade to a significant extent was STAT3; this confirms previous studies (*44*) and, together with the observation that gefitinib impairs activation of STAT5 (*45*), indicates that STAT modulation is a characteristic of EGFR-addicted cells not shared with Met-addicted cells. In sum, these results reinforce the notion that kinase inhibition

in addicted cells hits a subset of sensitive targets, while sparing other active, but apparently "proliferation" neutral, pathways.

At the transcriptional level, administration of 1 μM gefitinib, but not PHA, for 24 hours induced significant variations (fold change >2 and $P < 0.001$) in the expression of 1420 transcripts (749 up-regulated and 671 down-regulated; table S2). When comparing the transcriptional consequences of EGFR versus Met inhibition using the same high-stringency statistical filter, we found that 265 genes affected by gefitinib in DiFi (155 up-regulated and 110 down-regulated) were also significantly modulated by PHA in GTL16 cells (table S2), with a significant overlap between the two responses (Pearson correlation coefficient = 0.859, hypergeometric P value < 10^{-14}). A global survey of all the genes significantly modulated in either PHA-treated GTL16 or gefitinib-treated DiFi revealed an even more widespread similarity in the transcriptional profiles of the two cell lines, although the response of GTL16 to PHA was on the average less pronounced than that of DiFi to gefitinib (Fig. 3D and table S2). This suggests that, together with a significant core of co-regulated transcripts (265 genes), a subtle but broad relationship between the two transcriptional responses exists. To test this hypothesis in an unbiased manner, we considered all the transcripts expressed by both cell lines (8996 genes) and compared all the inhibitor-induced changes (including those below the statistical threshold) in a two-sample correlation plot (Fig. 3E): Even in the absence of gene selection, the two data sets displayed a significant correlation (Pearson correlation coefficient = 0.557, $P < 2.2 \times 10^{-16}$), confirming the broad overlap between the two responses. We subsequently filtered the 8996-gene group, using low stringency criteria for gene inclusion to identify a common response signature for EGFR-inhibited DiFi and Met-inhibited GTL16. The signature, composed of 1673 transcripts, and the selection criteria are illustrated in Fig. 3E. Moreover, GSEA analysis revealed that this co-regulated signature is highly enriched for five of the eight functionally important gene sets that we initially identified in inhibitor-treated GTL16 (Table 2).

In summary, this comparative analysis indicates that blockade of Met or EGFR in addicted cells impinges on common signaling pathways and involves a core of common transcriptional effectors, suggesting a stereotyped response that likely does not depend on receptor type or tissue origin. This mutuality supports the observation that *MET* gene amplification can substitute for EGFR activating mutations to convey growth signals and sustain tumorigenesis in gefitinib-resistant NSCLCs (*14*).

Inhibition of signals dependent on Ras or PI3K recapitulates the effects of Met inhibition

Our data suggest that when hyperactive tyrosine kinases are switched off, the ensuing biochemical and transcriptional response does not affect all of the pathways that are commonly governed by the inhibited or inactivated kinases. Instead, this response to kinase inhibition involves a specific and pathway-oriented complement of signal transducers and transcriptional effectors downstream of Ras or PI3K. Is this restricted complement sufficient to mediate the biological consequences of kinase inactivation, notwithstanding all the other pathways still operative in the cell? If Ras- and PI3K-regulated signals are the major, if not the exclusive, mediators of cell sensitivity to the growth and proliferation effects of receptor tyrosine kinase inhibition, then direct obstruction of such downstream signals should recapitulate the effects of upstream receptor inhibition. In animal models of K-Ras–driven lung adenocarcinomas, combined inhibition of PI3K and MEK leads to tumor regression (*46*). Accordingly, we forced a total abrogation of Ras- and PI3K-dependent effectors by treating a panel of Met-addicted cells with saturating concentrations of the MEK-specific inhibitor U0126 and the AKT-specific inhibitor Akt inhibitor X (AKTiX), either individually or in tandem. Working concentrations of the drugs were titrated in GTL16 cells by looking for complete depletion in the phosphorylated forms of MEK and AKT direct substrates—ERK1/2 for MEK and p70S6K for AKT (fig. S5). Indeed, inhibition of either MEK or AKT reduced GTL16 cell

proliferation (Fig. 4A), and simultaneous inactivation of the two pathways produced further reductions and substantially reproduced the effects of Met inhibition (Fig. 4A). We confirmed these results by performing single and combined treatments with two additional compounds against the same pathways, PD98059 (another MEK inhibitor) and LY294002 (a PI3K inhibitor) (Fig. 4A and fig. S5). In contrast, inhibition of p38 or JNK, kinases not modulated by Met inhibition, did not affect cell proliferation (Fig. 4B); consistently, p38 or JNK inactivation did not influence sensitivity to PHA (Fig. 4B).

We extended this analysis to the complement of Met-addicted cancer cells used for TaqMan validation, together with an additional NSCLC cell line featuring *MET* amplification, H1993 (*42*). In all cases, inhibition of either Ras- or PI3K-dependent signals decreased cell proliferation, which was more severely impaired by concurrent inhibition of both pathways (Fig. 4C). Together, these results corroborate the notion that cell-cycle arrest upon Met inactivation derives from the nullification of a small, but nonredundant, repertoire of Ras- and PI3K-dependent signals.

Active Ras or PI3K signals induce resistance to Met inhibition

The results with chemical inhibitors of Ras- and PI3K-dependent signals indicate that these pathways are necessary to fully sustain Met-dependent cell growth. To test if constitutive activation of such signals might suffice to decrease sensitivity to Met inhibitors, GTL16 cells were infected with an active mutant of K-RAS (K-RAS^{G12V}), B-RAF (B-RAF^{V600E}), which is activated by Ras and is the first kinase in the MEK-to-ERK MAPK pathway, and an active, myristoylated form of AKT (AKT^{Myr}), which is activated by PI3K, either singly or in combination, and cultured in the continuous presence of 0.5 μM PHA (Fig. 5A). As expected, proliferation of mock-infected cells was impeded by sustained Met inhibition; conversely, PHA-insensitive cells proliferated after individual expression of K-RAS^{G12V}, B-RAF^{V600E}, or AKT^{Myr} (Fig. 5B and fig. S6). The rescue effect of Ras was more pronounced than that of RAF or AKT even when cells were infected with both B-RAF^{V600E} and AKT^{Myr} (Fig. 5B and fig. S6). This stronger effect of Ras could be due to greater abundance of the mutant protein compared to that of the other two mutants (Fig. 5A) or may be due to signaling downstream of the constitutively active Ras that is independent of the pathways activated by Met.

Both B-RAF^{V600E} and AKT^{Myr} constructs contained a green fluorescent protein (GFP) reporter for monitoring transgene expression: Although immediately after viral transduction GFP-positive cells accounted for 15 to 25% of the total cell population, the percentage of GFP-positive cells reached 100% after 1 week of culture in the presence of PHA. Thence, Met inhibition exerted a positive selective pressure and led to the prevalence of resistant clones, expressing the active mutants. After PHA withdrawal for 48 hours, in a dose-response proliferation assay, cells coexpressing B-RAF^{V600E} and AKT^{Myr} proved to be completely insensitive to 0.05 μM PHA, a condition that induces a 50% proliferation suppression in mock cells; with increasing concentrations of PHA, resistant cells reached an inhibition plateau of only 35%, whereas mock cells abruptly displayed a 90% reduction in proliferation (Fig. 5C).

Ectopic expression of B-RAF^{V600E}, AKT^{Myr}, or both also conferred biochemical resistance. In cells expressing B-RAF^{V600E}, PHA-mediated inhibition of ERK1/2 phosphorylation was prevented and partial phosphorylation of the AKT substrate p70S6K was also retained. In cells expressing AKT^{Myr}, PHA-mediated down-regulation of p70S6K phosphorylation was blocked, without affecting PHA-mediated inhibition of ERK phosphorylation. The PHA-mediated reduction in the phosphorylation of ERK1/2 and p70S6K was partially counteracted by concomitant expression of both mutants (Fig. 6A). In these double transfectants, the modulation of gene expression induced by PHA treatment (1 μM; 24 hours of incubation after a 48-hour washout) was negligible (Fig. 6B and table S6). Almost all of the 581 genes belonging to the transcriptional response signature of wild-type GTL16

cells were either unaltered or exhibited subtle expression changes, with only 8 genes above the statistical threshold (fold change >2 and $P < 0.001$); when considering the whole transcriptome (24,000 genes), 11 genes were significantly changed by PHA treatment. The effects of exogenous introduction of K-RAS^{G12V} were similar to those observed in the B-RAF^{V600E}–AKT^{Myr} double transfectants. Met inhibition had only modest effects on the phosphorylation of both ERK1/2 and p70S6K (Fig. 6A). The gene expression profiles were also substantially unchanged: Only 12 genes of the transcriptional response signature and 40 genes in the global transcriptome were significantly modulated by Met blockade (Fig. 6B and table S6). Thus, cells in which Ras- or PI3K-dependent signals are hyperactive are globally refractory to Met inhibition, which is apparent at both the biochemical signaling and the transcriptional level.

To solidify the notion that active forms of RAF, AKT, or both produce resistance to Met inhibition, we extended the rescue experiments to the panel of *MET*-amplified, drug-sensitive cell lines used in the assays with MEK, PI3K, and AKT inhibitors. Similar to GTL16, introduction of either B-RAF^{V600E} or AKT^{Myr} established resistance in MKN45 and H1993; in HS746T, SNU5, and EBC1, we were able to obtain resistant clones from B-RAF^{V600E} transfectants, but not from cells expressing AKT^{Myr} (Fig. 7, A and B). Therefore, Ras- or PI3K-dependent signals act as functional response modifiers in several Met-addicted cancer cells of different tissue origin: Active RAF appears to be a “universal” determinant of resistance to Met inhibition, whereas active AKT displays a more restricted and context-specific activity. In those cell lines in which AKT activation is not sufficient to induce drug resistance, AKT blockade does decrease cell proliferation (Fig. 4C). This suggests that, in such contexts, the contribution of AKT to drug sensitivity might be important but not limiting.

Finally, to confirm the observation that Ras- or PI3K-dependent signals must be modulated by upstream receptor activity to ensure therapeutic efficacy, we genetically characterized by sequencing genes encoding several components of Ras- or PI3K-based pathways in the panel of Met-addicted cell lines. In these cells, the surveyed genes [*K-RAS*, *B-RAF*, *PIK3CA* (encoding the catalytic subunit of PI3K), and *PTEN*] appeared to be in their wild-type form, except for the *PIK3CA* gene in HS746T and H1993, which produces an E545A mutation in the protein (table S7). This mutation exhibits a weak oncogenic potency, compared with that of the “hotspot” mutation E545K, and does not sustain AKT activation in vivo (*47*, *48*). Consistently, we found that phosphorylation of AKT and p70S6K was inhibited by PHA treatment in both cell lines, indicating that this PI3K mutant is still responsive to upstream regulation (Fig. 7C). The lack of overt abnormalities in these genes in the Met-addicted cell lines tested provides a genetic proof of concept that the integrity of signals along the Ras and PI3K pathways is needed to ensure therapeutic responsiveness. EGFR-addicted DiFi cells also displayed wild-type forms of *K-RAS*, *B-RAF*, *PIK3CA*, and *PTEN* (table S7). This defines a common genetic background that is permissive for drug sensitivity and, once mutated, induces drug resistance.

DISCUSSION

It is well established that transient activation of receptor tyrosine kinases, for example, in response to short-term ligand stimulation, triggers a multitude of signaling pathways that act in concert to sustain cell survival and proliferation and to foster the malignant properties of cancer cells (*6*). Much less information is available about the opposite but complementary situation: What happens in the intracellular regulatory circuitry when a chronically hyperactive receptor tyrosine kinase that drives proliferation and survival of a given tumor is abruptly switched off, leading to the induction of cell-cycle arrest or cell death? Intuitively, if receptor deregulated activity prevails over the many concurrent abnormalities that are normally operative in a full-blown tumor, all the signals emanated

by this “dominant” oncoprotein would be expected to be silenced upon receptor inactivation, and this global signal obliteration would provoke growth inhibition or apoptosis.

The major downstream signals triggered by the receptor tyrosine kinase Met and involved in Met mitogenic, antiapoptotic, or transforming abilities include several signaling cascades and components: the Ras-RAF-MEK-ERK and PI3K-AKT axes, STATs, NF-κB, and MAPKs of the JNK and p38 families (*22–24*, *26–32*). In cancer cells naturally featuring continuous Met hyperactivation and addicted to Met for sustained proliferation, we found that Met inhibition did not lead to a generalized deactivation of all these signaling pathways; instead, receptor inhibition specifically decreased a limited signature of Ras-dependent and PI3K-dependent transducers and transcriptional regulators. Although phosphoproteomic and transcriptional analyses were performed at a single time point (2 and 24 hours, respectively), the results indicate that the effects of Met inactivation (namely, cell-cycle arrest) can be recapitulated by blocking the major components of the Ras or PI3K transduction cascades, and resistance to Met inhibition can be produced by active mutants of components in those cascades. Interestingly, constitutive activation of signals downstream of Ras or PI3K in Met-addicted cells not only overrides the proliferative block caused by Met inactivation but also severely dampens the transcriptional response to Met inhibition, pointing to a specific role for Ras and PI3K pathways in mediating the biological consequences of Met neutralization. Thus, components in pathways other than those downstream of Ras or PI3K exhibited no change in response to Met inhibition and this lack of signal modification resulted in lack of functional responses. For example, inactivation of either JNK or p38, which showed little or no response to Met blockade, did not influence the proliferation of Met-addicted cancer cells.

This signaling and functional dichotomy between “sensitive” and “indifferent” pathways occurs only in Met-addicted cancer cells, in which Met constitutive activation is integral to the natural history of the tumor cells and represents the driving force for maintaining the transformed phenotype. When Met activation is imposed exogenously—by either ligand stimulation or Met ectopic overexpression—in cells in which Met is basally inactive, then HGF-dependent proliferation and survival are impaired by PI3K or ERK inhibition (*23*, *24*), which is the same as the Met-addicted cells. In contrast, individual inhibition of the signals that are “indifferent” in the Met-addicted cells—JNK, p38, STATs, and NF-κB—can also adversely affect Met-driven cell proliferation in various cell types and under different experimental settings (*27–32*). This suggests that although Met-dependent proliferation in response to external stimuli can be controlled by many different pathways, inherent addiction to Met for continuous growth is governed by a restricted compendium of signal transducers. Several hypotheses may explain why the indifferent pathways display slight or no changes in response to Met inhibition. One possibility is that such signals have undergone desensitization as a consequence of adaptive mechanisms engaged in response to long-term Met hyperactivity (*1*, *7*); alternatively, these pathways could be indirectly sustained by compensatory feed-back circuits (*8*).

Phosphoprotein and gene expression profiling revealed that EGFR inactivation in EGFR-addicted cells leads to response signatures similar to those of Met-inactivated, Met-addicted cells, indicating that tumor dependence on deregulated kinase activity of either receptor is controlled by a subset of common signaling pathways and involves a core of common transcriptional effectors. This observation suggests that cancer cells addicted to receptor tyrosine kinases develop stereotyped systems to sustain their malignant behavior and that drug sensitivity or resistance is determined by widely shared mechanisms, independent of the molecular identity of the addictive kinase. Consistent with this and similar to our findings, a genome-wide loss-of-function screen has demonstrated that hyperactivation of PI3K-dependent signals induces resistance to HER2 inhibitors in breast cancer (*49*). The role of Ras signaling and PI3K signaling as the major and possibly sole determinants of drug sensitivity may well extend to molecules different from tyrosine

kinases; for example, the antiproliferative effects of estrogen inhibition can be circumvented by hyperactivation of RAF and consequent stimulation of the ERK pathway (*50*). One caveat of all these studies, including ours, is the use of immortalized cell lines, which display a genetic drift and a biological compliance different from human cancers in vivo as a consequence of cellular adaptation to tissue-culture conditions. However, the information from in vitro approaches is supported clinically by a series of retrospective investigations on patients treated with EGFR inhibitors, according to which aberrant activation of Ras and Ras-based signals (for example, RAF mutations) is associated with poor clinical outcome (*51–53*). We expect that such predictive determinants of therapeutic response will also apply to Met-targeted therapies, which are now in early-phase clinical trials.

Met inhibition in Met-addicted cancer cells leads to cell-cycle arrest rather than apoptosis (at least in the prototypic GTL16 model). This suggests that therapies targeting only Met may be insufficient to induce tumor shrinkage—even in a clinical context of overt Met-addiction—and advocates for the use of therapies that might in combination with Met inhibitors produce a cytotoxic effect. One should also consider that Met activity protects against proapoptotic chemotherapeutics (*54–57*), which offers a rationale for the combined use of standard chemotherapy and Met-targeted therapy to increase (or reinstate) chemosensitivity. Moreover, the cytostatic activity of Met inhibitors is likely to allow the persistence of cancer cells that are quiescent but alive. This, together with the selective pressure exerted by prolonged therapies targeting Met, could favor the emergence of clones with randomly activated rescue pathways (for example, Ras, RAF, or PI3K mutations). Again, a multidrug approach with other targeting agents (for example, compounds that block Met downstream effectors, such as rapamycin analogs or MEK inhibitors) might obviate this drawback.

In summary, our data indicate that short-term receptor inhibition under conditions of long-term receptor hyperactivity does not lead to a global silencing of the all cellular regulatory circuits downstream of the hyperactive receptor; instead, receptor inactivation nullifies a small but functionally important complement of cascades involving Ras and PI3K, and this signal abrogation is necessary and sufficient to stop proliferation of cancer cells. The mechanisms whereby, after inhibition of oncogene activity, other pathways remain substantially unaltered and do not contribute to the inhibition of cellular proliferation remain ground for future studies. That cells addicted to receptor tyrosine kinases rely on a restricted cadre of signaling effectors to encourage tumor proliferation unveils an Achilles' heel in oncogene-addicted tumors. Ras effector and PI3K effectors may be the critical vulnerabilities of such tumors, despite the many genetic and epigenetic insults that earmark malignancy and the persistence of several other "active" signals.

MATERIALS AND METHODS

Cell lines, compounds, antibodies, vectors, and viral infection

GTL16, MKN45, and H1993 cells were maintained in RPMI 1640; EBC1, SNU5 and HS746T in Iscove; DiFi cells (from J. Baselga, Vall d'Hebron University, Barcelona, Spain) were cultured in F12. PHA-665752 and gefitinib were synthesized at the Servier Research Institute (France) on the basis of the available chemical structures. All other pharmacologic inhibitors were from Calbiochem. The following antibodies were used: antibody against human Met (Upstate Biotechnology); antibody against phosphorylated Met ($Tyr^{1234/1235}$), antibody against phosphorylated ERK (Thr^{202}/Tyr^{204}), antibody against total ERK, antibody against phosphorylated AKT (Ser^{473}), antibody against total AKT, antibody against phosphorylated p70S6K (Thr^{421}/Ser^{424}) (Cell Signaling); antibody against B-RAF (Santa Cruz Biotechnology); antibody against K-, H-, and N-Ras (Calbiochem); and antibody against vinculin (Sigma). The $B\text{-}RAF^{V600E}$ and the $K\text{-}RAS^{G12V}$ lentiviral vectors were from M. Soengas (University of Michigan, Ann Arbor, MI) and F.

d'Adda di Fagagna [FIRC Institute of Molecular Oncology (IFOM), Milan, Italy], respectively; the AKT^{Myr} retroviral vector was from L. Primo (IRCC, Turin, Italy). The doxycycline-inducible short hairpin RNA (shRNA) against Met has been previously described (*19*). Viral vectors were produced by lipofectAMINE 2000 (Invitrogen)–mediated transient transfection of 293T (for lentiviruses) or Phoenix cells (for retroviruses).

Cell proliferation (viability) assays and cell-cycle analysis

Proliferative response was measured with an ATP content assay as an indicator of cellular viability. On day 0, 1000 cells were resuspended in 50 µl of complete growth medium and seeded in 96-well plastic culture plates. On day 1, 50 µl of drugs or vehicle serially diluted in complete medium were added to cells. On day 5, cell viability was assessed by ATP content with a luminescence assay (ATPlite 1 step kit, Perkin Elmer). All measurements were recorded with a DTX 880-Multimode plate reader (Beckman-Coulter). Proliferation inhibition at each drug concentration was normalized to vehicle-treated cells. In some experiments, cell numbers were measured every 4 days for 16 days.

For cell-cycle analysis, untreated and drug-treated cells were harvested and stained with propidium iodide with the DNAcon3 kit (Consul T.S.), according to the manufacturer's instructions. Detection and quantification of sub-G_1, G_1, and S populations were performed by flow cytometric analysis.

Multiplex phosphoproteomics

In Luminex (BioPLex, Biorad) analysis, individual color-coded (fluorescently dyed) microspheres were conjugated with a specific capture antibody against a given transducer. Conjugated bead mixtures were incubated with cell lysates and with fluorescently labeled reporter antibodies in a sandwich immunoassay performed in microplate wells. The constituents of each well were drawn into a flow-based array reader, which identified each specific reaction on the basis of bead color and quantified the result. The magnitude of the reaction was measured as the intensity of the fluorescently labeled reporter antibodies. Information on the antibodies used for Luminex analysis are in table S1. MesoScale Discovery (MSD) is a solid-phase multiarray technology in which multiple capture antibodies are immobilized onto single microplate wells. After incubation with protein extracts, detection was performed by quantitative electrochemiluminescence with reporter antibodies coupled with SULFO-TAG, an amine-reactive, *N*-hydroxysuccinimide ester that emits light upon electrochemical stimulation. Information on the kits used is available in table S1 and on http://www.mesoscale.com. ELISA assays (PathScan, Cell Signaling) were performed according to the manufacturer's instructions.

For all analyses, cells were either left untreated or treated with 0.4 µM PHA or gefitinib for 2 hours. When inducible shRNAs were used, cell lysis was performed 48 hours after doxycycline addition. Each experimental point consisted of lysates (2 ml) from 20×10^6 cells. Protein extraction was performed with the Bio-Plex cell lysis kit (Biorad) for Luminex and with the MSD tris lysis buffer [150 mM NaCl, 20 mM tris (pH 7.5), 1 mM EDTA, 1 mM EGTA, 1% Triton X-100] for MSD.

Western blotting

Proteins were extracted with MSD tris lysis buffer. Extracts were clarified at 12,000 rpm for 15 min and normalized with the BCA Protein Assay Reagent Kit. Proteins were electrophoresed on SDS–polyacrylamide gels and transferred onto nitrocellulose membranes (Hybond, Amersham). Nitrocellulose-bound antibodies were detected by the enhanced chemiluminescence system (ECL, Amersham).

cDNA microarrays, GSEA analysis, TaqMan low-density array qPCR, and sequencing

Total RNA was isolated with TRIzol (Invitrogen). For microarray analysis, reverse transcription and biotinylated complementary RNA (cRNA) synthesis were performed with the Illumina TotalPrep RNA Amplification Kit (Ambion). Hybridization of the cRNAs was performed on Sentrix HumanRef-8_v2 Expression BeadChips (24K, Illumina). Hybridized arrays were stained and scanned in a Beadstation 500 (Illumina). BeadStudio software (Illumina) was used to analyze raw data grouped by experimental condition. After rank-invariant normalization, genes were filtered for detection (>0.95 for all the experimental groups) and assessed for statistically significant differential expression with the Illumina custom test (iterative robust least-squares fit). According to this test, a differential score higher than 30 corresponds to $P < 0.001$.

GSEA was performed with the publicly available desktop application from the Broad Institute (http://www.broadinstitute.org/gsea/msigdb/downloads.jsp). Genes represented by more than one probe were collapsed with the XCollapseProbes utility to the probe with the maximum value. We used the gene sets database of curated sets, c2.v2.symbols.gmt. Because of the small number of samples, *P* values were calculated by repeating gene permutations 1000 times. Enrichment statistics were performed with the default setting.

For TaqMan low-density array qPCR, complementary DNA (cDNA) was prepared with the High Capacity cDNA Reverse Transcription Kit (Applied Biosystems). TaqMan qPCR reactions targeted the 48 genes chosen among the transcriptional response signature and a reference gene (*POLR2A*) in a microfluidic card.

For sequencing analysis, genomic DNA was extracted with the Wizard Purification System (Promega). Exon-specific and sequencing primers were designed with Primer3 software and synthesized by Sigma. Purified PCR products were sequenced with BigDye Terminator version 3.1 Cycle Sequencing kit (Applied Biosystems) and analyzed with a 3730 ABI capillary electrophoresis system.

The array data have been deposited in the National Center for Biotechnology Information Gene Expression Omnibus (GEO; http://www.ncbi.nlm.nih.gov/geo/) and are accessible through GEO Series accession number GSE19043.

Acknowledgments

We thank A. Bardelli, J. Baselga, C. Boccaccio, C. Bracco, D. Cantarella, F. d'Adda di Fagagna, L. Di Blasio, F. Di Nicolantonio, P. Gagliardi, A. Galati, C. Isella, S. Lamba, B. Martinoglio, P. Michieli, L. Primo, M. Soengas, and C. Zanon for help with the experiments, discussion, and sharing reagents; R. Albano, S. Giove, and L. Palmas for technical assistance; and A. Cignetto for secretarial assistance. This work was funded by Institut de Recherches Servier and by grants from Associazione Italiana per la Ricerca sul Cancro (AIRC), Regione Piemonte, and Ministero dell'Università e della Ricerca to P.M.C., S.G., E.M., and L.T.; European Union FP6 and FP7, Compagnia di San Paolo, and Fondazione CRT to P.M.C. A.B. is the recipient of an AIRC fellowship.

Supplementary Materials

Fig. S1. Validation of phosphoprotein antibodies for multiplex phosphoproteomic analysis.

Fig. S2. Met inhibition has little or no effects on the activation of p38 MAPK, JNK, STAT3, and NF-κB.

Fig. S3. Met inhibition neutralizes the activity of AKT and ERK1/2.

Fig. S4. Microarray validation by TaqMan low-density quantitative PCR arrays.

Fig. S5. Effects of MEK, PI3K, and AKT inhibitors on downstream effectors in GTL16 cells.

Fig. S6. Basal proliferation curves of PHA-resistant GTL16 cells.

Table S1. Phosphoproteomic analysis of cell lines treated with PHA or gefitinib.
Table S2. Transcriptional profiles of GTL16 and DiFi cells treated with PHA or gefitinib.
Table S3. Functional annotation analysis of genes significantly downregulated by PHA in GTL16 cells.
Table S4. Gene set enrichment analysis (GSEA) results for Genesets downregulated by PHA in GTL16 cells.
Table S5. TaqMan validation of the transcriptional response to Met inhibition in Met-amplified cell lines.
Table S6. Transcriptional profiles of control GTL16 (mock), GTL16 expressing B-RAF^{V600E} and AKT^{Myr}, and GTL16 expressing K-RAS^{G12V} treated with PHA.
Table S7. Mutational analysis of Met- and EGFR-addicted cell lines.

REFERENCES AND NOTES

1. S. V. Sharma, J. Settleman, Oncogene addiction: Setting the stage for molecularly targeted cancer therapy.Genes Dev. 21, 3214–3231 (2007).
2. R. S. Herbst, M. Fukuoka, J. Baselga, Gefitinib—a novel targeted approach to treating cancer. Nat. Rev. Cancer 4, 956–965 (2004).
3. R. Ren, Mechanisms of BCR-ABL in the pathogenesis of chronic myelogenous leukaemia. Nat. Rev. Cancer5, 172–183 (2005).
4. S. V. Sharma, D. W. Bell, J. Settleman, D. A. Haber, Epidermal growth factor receptor mutations in lung cancer. Nat. Rev. Cancer 7, 169–181 (2007).
5. K. Imai, A. Takaoka, Comparing antibody and small-molecule therapies for cancer. Nat. Rev. Cancer 6,714–727 (2006).
6. J. Schlessinger, Cell signaling by receptor tyrosine kinases. Cell 103, 211–225 (2000).
7. A. Kamb, Consequences of nonadaptive alterations in cancer. Mol. Biol. Cell 14, 2201–2205 (2003).
8. I. Amit, A. Citri, T. Shay, Y. Lu, M. Katz, F. Zhang, G. Tarcic, D. Siwak, J. Lahad, J. JacobHirsch, N.Amariglio, N. Vaisman, E. Segal, G. Rechavi, U. Alon, G. B. Mills, E. Domany, Y. Yarden, A module of negative feedback regulators defines growth factor signaling. Nat. Genet. 39, 503–512 (2007).
9. K. Rikova, A. Guo, Q. Zeng, A. Possemato, J. Yu, H. Haack, J. Nardone, K. Lee, C. Reeves, Y. Li, Y. Hu,Z. Tan, M. Stokes, L. Sullivan, J. Mitchell, R. Wetzel, J. Macneill, J.M. Ren, J. Yuan, C.E. Bakalarski, J.Villen, J.M. Kornhauser, B. Smith, D. Li, X. Zhou, S.P. Gygi, T.L. Gu, R.,D. Polakiewicz, J. Rush, M. J.Comb, Global survey of phosphotyrosine signalling identifies oncogenic kinases in lung cancer. Cell 131,1190–1203 (2007).
10. P. M. Comoglio, S. Giordano, L. Trusolino, Drug development of MET inhibitors: Targeting oncogene addiction and expedience. Nat. Rev. Drug Discov. 7, 504–516 (2008).
11. G.A. Smolen, R. Sordella, B. Muir, G. Mohapatra, A. Barmettler, H. Archibald, W.J. Kim, R.A. Okimoto, D.W. Bell, D.C. Sgroi, J.G. Christensen, J. Settleman, D.A. Haber, Amplification of MET may identify a subset of cancers with extreme sensitivity to the selective tyrosine kinase inhibitor PHA-665752. Proc. Natl. Acad. Sci. U.S.A. 103, 2316–2321 (2006).
12. U. McDermott, S.V. Sharma, L. Dowell, P. Greninger, C. Montagut, J. Lamb, H. Archibald, R. Raudales,A. Tam, D. Lee, S.M. Rothenberg, J.G. Supko, R. Sordella, L.E. Ulkus, A.J. Iafrate, S. Maheswaran, C.N.Njauw, H. Tsao, L. Drew, J.H. Hanke, X.J. Ma, M.G. Erlander, N.S. Gray, D.A. Haber, J. Settleman,Identification of genotype-correlated sensitivity to selective kinase inhibitors by using high-throughput tumor cell line profiling. Proc. Natl. Acad. Sci. U.S.A. 104, 19936–19941 (2007).

13.J. Bean, C. Brennan, J.Y. Shih, G. Riely, A. Viale, L. Wang, D. Chitale, N. Motoi, J. Szoke, S. Br oderick,M. Balak, W.C. Chang, C. J. Yu, A. Gazdar, H. Pass, V. Rusch, W. Gerald, S. F. Huang, P. C. Yang, V.Miller, M. Ladanyi, C. H. Yang, W. Pao, MET amplification occurs with or without T790M mutations in EGFR mutant lung tumors with acquired resistance to gefitinib or erlotinib. Proc. Natl. Acad. Sci. U.S.A. 104,20932–20937 (2007).
14. J. A. Engelman, K. Zejnullahu, T. Mitsudomi, Y. Song, C. Hyland, J. O. Park, N. Lindeman, C. M. Gale, X.Zhao, J. Christensen, T. Kosaka, A.J. Holmes, A.M. Rogers, F. Cappuzzo, T. Mok, C. Lee, B.E. Johnson,L.C. Cantley, P.A. Jänne, MET amplification leads to gefitinib resistance in lung cancer by activating ERBB3 signaling. Science 316, 1039–1043 (2007).
15. L. V. Sequist, R. G. Martins, D. Spigel, S. M. Grunberg, A. Spira, P. A. Jänne, V. A. Joshi, D. McCollum, T.L. Evans, A. Muzikansky, G.L. Kuhlmann, M. Han, J.S. Goldberg, J. Settl eman, A. J. Iafrate, J. A.Engelman, D. A. Haber, B. E. Johnson, T. J. Lynch, First-line gefitinib in patients with advanced non-small-cell lung cancer harboring somatic EGFR mutations. J. Clin. Oncol. 26, 2442–2449 (2008).
16. J. G. Christensen, J. Burrows, R. Salgia, c-Met as a target for human cancer and characterization of inhibitors for therapeutic intervention. Cancer Lett. 225, 1–26 (2005).
17. B. Peruzzi, D. P. Bottaro, Targeting the c-Met signaling pathway in cancer. Clin. Cancer Res. 12, 3657–3660(2006)
18. B. S. Knudsen, G. Vande Woude, Showering c-MET-dependent cancers with drugs. Curr. Opin. Genet. Dev.18, 87–96 (2008).
19. S. Corso, C. Migliore, E. Ghiso, G. De Rosa, P. M. Comoglio, S. Giordano, Silencing the MET oncogene leads to regression of experimental tumors and metastases. Oncogene 27, 684–693 (2008).
20. J. Herrick, X. Michalet, C. Conti, C. Schurra, A. Bensimon, Quantifying single gene copy number by measuring fluorescent probe lengths on combed genomic DNA. Proc. Natl. Acad. Sci. U.S.A. 97, 222–227(2000).
21. J.
G. Christensen, R. Schreck, J. Burrows, P. Kuruganti, E. Chan, P. Le, J. Chen, X. Wang, L. Ruslim R.Blake, K. E. Lipson, J. Ramphal, S. Do, J. J. Cui, J. M. Cherrington, D. B. Mendel, A selective small molecule inhibitor of c-Met kinase inhibits c-Met-dependent phenotypes in vitro and exhibits cytoreductive antitumor activity in vivo. Cancer Res. 63, 7345–7355 (2003).
22. P.C. Ma, M.S. Tretiakova, V. Nallasura, R. Jagadeeswaran, A.N. Husain, R. Salgia, Downstrea m signalling and specific inhibition of c-MET/HGF pathway in small cell lung cancer: Implications for tumour invasion. Br. J. Cancer 97, 368–377 (2007).
23. N. Rahimi, E. Tremblay, B. Elliott, Phosphatidylinositol 3-kinase activity is required for hepatocyte growth factor-induced mitogenic signals in epithelial cells. J. Biol. Chem. 271, 24850–24855 (1996).
24. G. H. Xiao, M. Jeffers, A. Bellacosa, Y. Mitsuuchi, G. F. Vande Woude, J. R. Testa, Anti-apoptotic signaling by hepatocyte growth factor/Met via the phosphatidylinositol 3-kinase/Akt and mitogen-activated protein kinase pathways. Proc. Natl. Acad. Sci. U.S.A. 98, 247–252 (2001).
25. A. Guo, J. Villén, J. Kornhauser, K.A. Lee, M.P. Stokes, K. Rikova, A. Possemato, J. Nardone, G.Innocenti, R. Wetzel, Y. Wang, J. MacNeill, J. Mitchell, S.P. Gygi, J. Rush, R.D. Polakiewicz, M. J. Comb, Signaling networks assembled by oncogenic EGFR and c-Met. Proc. Natl. Acad. Sci. U.S.A. 105, 692–697(2008).
26. C. Ponzetto, A. Bardelli, Z. Zhen, F. Maina, P.DallaZonca, S. Giordano, A. Graziani, G. Panayo tou, P. M.Comoglio, A multifunctional docking site mediates signaling and transformation by the hepatocyte growth factor/scatter factor receptor family. Cell 77, 261–271 (1994).
27. G. A. Rodrigues, M. Park, J. Schlessinger, Activation of the JNK pathway is essential for transformation by the Met oncogene. EMBO J. 16, 2634–2645 (1997).

28.C. Boccaccio, M. Andò, L. Tamagnone, A. Bardelli, P. Michieli, C. Battistini, P.M. Comoglio, Induction of epithelial tubules by growth factor HGF depends on the STAT pathway. Nature 391, 285–288 (1998).
29.K.L. Auer, J. Contessa, S. BrenzVerca, L. Pirola, S. Rusconi, G. Cooper, A. Abo, M.P. Wymann , R. J.Davis, M. Birrer, P. Dent, The Ras/Rac1/Cdc42/SEK/JNK/c-Jun cascade is a key pathway by which agonists stimulate DNA synthesis in primary cultures of rat hepatocytes. Mol. Biol. Cell 9, 561–573 (1998).
30. M. Garcia-Guzman, F. Dolfi, K. Zeh, K. Vuori, Met-induced JNK activation is mediated by the adapter protein Crk and correlates with the Gab1 - Crk signaling complex formation. Oncogene 18, 7775–7786 (1999).
31. M. Müller, A. Morotti, C. Ponzetto, Activation of NF-κB is essential for hepatocyte growth factor-mediated proliferation and tubulogenesis. Mol. Cell. Biol. 22, 1060–1072 (2002).
32. J. A. Recio, G. Merlino, Hepatocyte growth factor/scatter factor activates proliferation in melanoma cells through p38 MAPK, ATF-2 and cyclin D1. Oncogene 21, 1000–1008 (2002).
33. G. Dennis Jr, B.T. Sherman, D.A. Hosack, J. Yang, W. Gao, H.C. Lane, R.,A. Lempicki, DAVID: Database for Annotation, Visualization, and Integrated Discovery. Genome Biol. 4, P3 (2003).
34. A. Subramanian, P. Tamayo, V.K. Mootha, S. Mukherjee, B.L. Ebert, M.A. Gillette, A. Paulovic h, S. L.Pomeroy, T. R. Golub, E. S. Lander, J. P. Mesirov, Gene set enrichment analysis: A knowledge-based approach for interpreting genome-wide expression profiles. Proc. Natl. Acad. Sci. U.S.A. 102, 15545–15550(2005).
35. V.K. Mootha, C.M. Lindgren, K.F. Eriksson, A. Subramanian, S. Sihag, J. Lehar, P. Puigserver, E.Carlsson, M. Ridderstråle, E. Laurila, N. Houstis, M.J. Daly, N. Patterson, J. P. Mesirov, T. R. Golub, P.Tamayo, B. Spiegelman, E. S. Lander, J. N. Hirschhorn, D. Altshuler, L. C. Groop, PGC-1α-responsive genes involved in oxidative phosphorylation are coordinately downregulated in human diabetes. Nat. Genet. 34,267–273 (2003).
36. I. Vivanco, N. Palaskas, C. Tran, S.P. Finn, G. Getz, N.J. Kennedy, J. Jiao, J. Rose, W. Xie, M. Loda, T.Golub, I. K. Mellinghoff, R. J. Davis, H. Wu, C. L. Sawyers, Identification of the JNK signaling pathway as a functional target of the tumor suppressor PTEN. Cancer Cell 11, 555–569 (2007).
37. M. Schuhmacher, F. Kohlhuber, M. Hölzel, C. Kaiser, H. Burtscher, M. Jarsch, G. W. Bornkamm, G. Laux,A. Polack, U. H. Weidle, D. Eick, The transcriptional program of a human B cell line in response to Myc. Nucleic Acids Res. 29, 397–406 (2001).
38. H. Y. Chang, J. B. Sneddon, A. A. Alizadeh, R. Sood, R. B. West, K. Montgomery, J. T. Chi, M. van de Rijn, D. Bolstein, P. O. Brown, Gene expression signature of fibroblast serum response predicts human cancer progression: Similarities between tumors and wounds. PLoS Biol. 2, E7 (2004).
39. B. Ren, H. Cam, Y. Takahashi, T. Volkert, J. Terragni, R. A. Young, B. D. Dynlacht, E2F integrates cell cycle progression with DNA repair, replication, and G_2/M checkpoints. Genes Dev. 16, 245–256 (2002).
40. A. Sweet-Cordero, S. Mukherjee, A. Subramanian, H. You, J.J. Roix, C. Ladd-Acosta, J. Mesirov, T. R.Golub, T. Jacks, An oncogenic KRAS2 expression signature identified by cross-species gene-expression analysis. Nat. Genet. 37, 48–55 (2005).
41. T. Peng, T. R. Golub, D. M. Sabatini, The immunosuppressant rapamycin mimics a starvation-like signal distinct from amino acid and glucose deprivation. Mol. Cell. Biol. 22, 5575–5584 (2002).
42. B. Lutterbach, Q. Zeng, L. J. Davis, H. Hatch, G. Hang, N. E. Kohl, J. B. Gibbs, B. S. Pan, Lung cancer cell lines harboring *MET* gene amplification are dependent on Met for growth and survival. Cancer Res. 67,2081–2088 (2007).

43. J. Albanell, J. CodonyServat, F. Rojo, J.M. DelCampo, S. Sauleda, J. Anido, G. Raspall, J. Gira lt, J.Roselló, R. I. Nicholson, J. Mendelsohn, J. Baselga, Activated extracellular signal-regulated kinases: Association with epidermal growth factor receptor/transforming growth factor α expression in head and neck squamous carcinoma and inhibition by anti-epidermal growth factor receptor treatments. Cancer Res. 61,6500–6510 (2001).
44. J. Albanell, F. Rojo, J. Baselga, Pharmacodynamic studies with the epidermal growth factor receptor tyrosine kinase inhibitor ZD1839. Semin. Oncol. 28, 56–66 (2001).
45. S. V. Sharma, P. Gajowniczek, I. P. Way, D. Y. Lee, J. Jiang, Y. Yuza, M. Classon, D. A. Haber, J.Settleman, A common signaling cascade may underlie "addiction" to the Src, BCR-ABL, and EGF receptor oncogenes. Cancer Cell 10, 425–435 (2006).
46. J.A. Engelman, L. Chen, X. Tan, K. Crosby, A.R. Guimaraes, R. Upadhyay, M. Maira, K. McNa mara, S. A. Perera, Y. Song, L. R. Chirieac, R. Kaur, A. Lightbown, J. Simendinger, T. Li, R. F. Padera, C. García-Echeverría, R. Weissleder, U. Mahmood, L. C. Cantley, K. K. Wong, Effective use of PI3K and MEK inhibitors to treat mutant Kras G12D and PIK3CA H1047R murine lung cancers. Nat. Med. 14, 1351–1356 (2008).
47. P. K. Vogt, S. Kang, M. A. Elsliger, M. Gymnopoulos, Cancer-specific mutations in phosphatidylinositol 3-kinase. Trends Biochem. Sci. 32, 342–349 (2007).
48. S. Kang, S. S. Seo, H. J. Chang, C. W. Yoo, S. Y. Park, S. M. Dong, Mutual exclusiveness between PIK3CA and KRAS mutations in endometrial carcinoma. Int. J. Gynecol. Cancer 18, 1339–1343 (2008).
49. K. Berns, H. M. Horlings, B. T. Hennessy, M. Madiredjo, E. M. Hijmans, K. Beelen, S. C. Linn, A. M.Gonzalez-Angulo, K. Stemke-Hale, M. Hauptmann, R. L. Beijersbergen, G. B. Mills, M. J. van de Vijver, R.Bernards, A functional genetic approach identifies the PI3K pathway as a major determinant of trastuzumab resistance in breast cancer. Cancer Cell 12, 395–402 (2007).
50. E. Iorns, N. C. Turner, R. Elliott, N. Syed, O. Garrone, M. Gasco, A. N. J. Tutt, T. Crook, C. J. Lord, A.Ashworth, Identification of CDK10 as an important determinant of resistance to endocrine therapy for breast cancer. Cancer Cell 13, 91–104 (2008).
51. J. Baselga, N. Rosen, Determinants of RASistance to anti-epidermal growth factor receptor agents. J. Clin. Oncol. 26, 1582–1584 (2008).
52. C. S. Karapetis, S. Khambata-Ford, D. J. Jonker, C. J. O'Callaghan, D. Tu, N. C. Tebbutt, R. J. Simes, H.Chalchal, J. D. Shapiro, S. Robitaille, T. J. Price, L. Shepherd, H. J. Au, C. Langer, M. J. Moore, J. R.Zalcberg, *K-ras* mutations and benefit from cetuximab in advanced colorectal cancer. N. Engl. J. Med. 359,1757–1765 (2008).
53. F. Di Nicolantonio, M. Martini, F. Molinari, A. Sartore-Bianchi, S. Arena, P. Saletti, S. De Dosso, L.Mazzucchelli, M. Frattini, S. Siena, A. Bardelli, Wild-type *BRAF* is required for response to panitumumab or cetuximab in metastatic colorectal cancer. J. Clin. Oncol. 26, 5705–5712 (2008).
54. S. Fan, J. A. Wang, R. Q. Yuan, S. Rockwell, J. Andres, A. Zlatapolskiy, I. D. Goldberg, E. M. Rosen,Scatter factor protects epithelial and carcinoma cells against apoptosis induced by DNA-damaging agents.Oncogene 17, 131–141 (1998).
55. S. Fan, Y. X. Ma, J. A. Wang, R. Q. Yuan, Q. Meng, Y. Cao, J. J. Laterra, I. D. Goldberg, E. M. Rosen, The cytokine hepatocyte growth factor/scatter factor inhibits apoptosis and enhances DNA repair by a common mechanism involving signaling through phosphatidyl inositol 3′ kinase. Oncogene 19, 2212–2223 (2000).
56. Q. Meng, J. M. Mason, D. Porti, I. D. Goldberg, E. M. Rosen, S. Fan, Hepatocyte growth factor decreases sensitivity to chemotherapeutic agents and stimulates cell adhesion, invasion, and migration. Biochem. Biophys. Res. Commun. 274, 772–779 (2000).

57. D.C. Bowers, S. Fan, K.A. Walter, R. Abounader, J.A. Williams, E.M. Rosen, J. Laterra, Scatter factor/hepatocyte growth factor protects against cytotoxic death in human glioblastoma via phosphatidylinositol 3-kinase- and AKT-dependent pathways. Cancer Res. 60, 4277–4283 (2000).

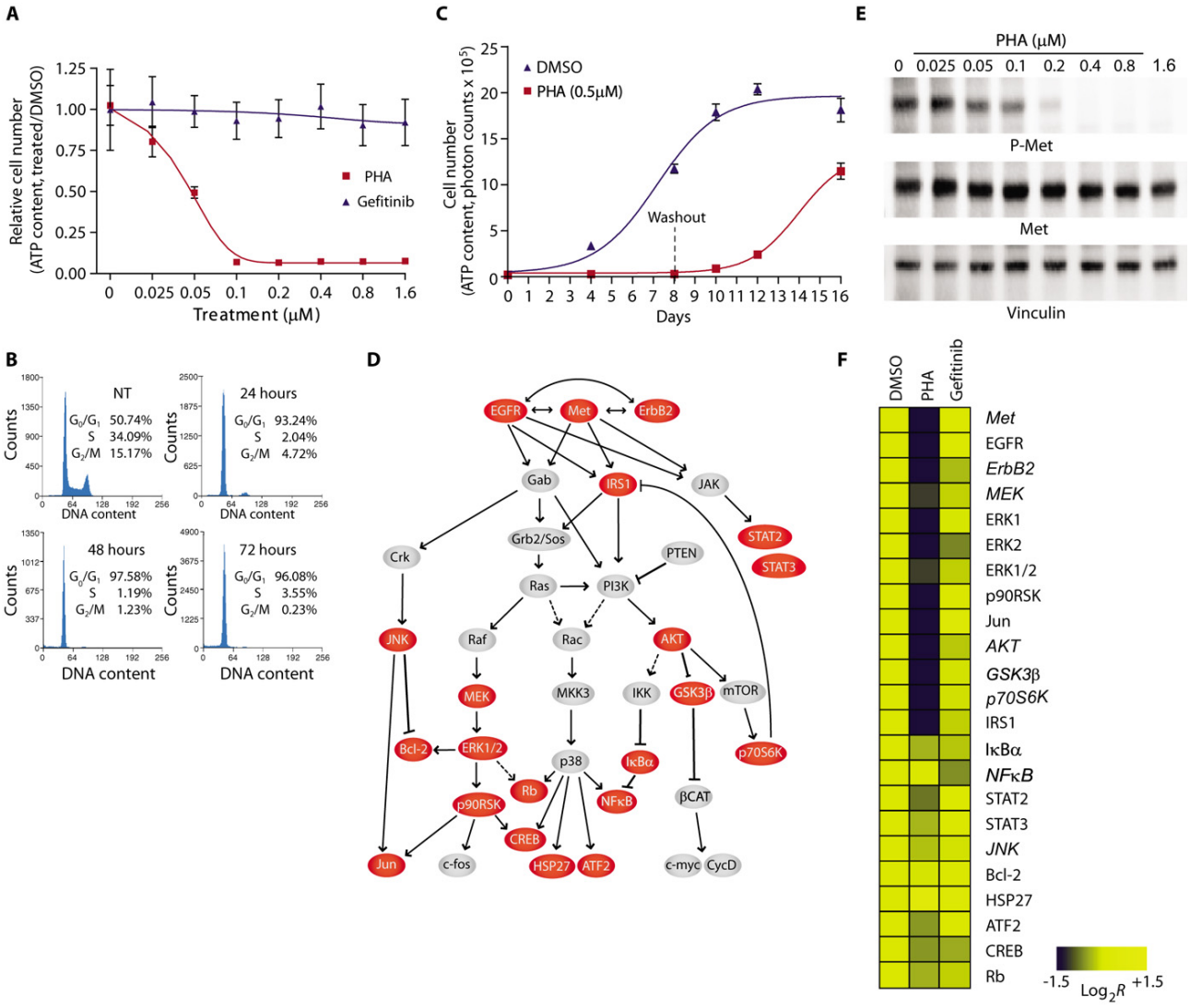

Figure 1. Met inhibition modulates the activity of Ras-PI3K–dependent signals. (A) Inhibition of proliferation in GTL16 cells treated for 96 hours with increasing concentrations of the Met inhibitor PHA-665752 (PHA). The EGFR inhibitor gefitinib is ineffective. Data are the means ± SD of eight samples (two independent experiments performed in quadruplicate). DMSO, dimethyl sulfoxide. (B) Cell-cycle analysis of GTL16 untreated (NT) or treated with PHA for 24, 48, and 72 hours. (C) Proliferation of GTL16 in the presence or absence of PHA. In the PHA-treated cells, the inhibitor was removed after eight days (washout). Data are the means ± SD of eight samples (two independent experiments performed in quadruplicate). (D) Interaction map of Met downstream signaling, according to published data. Red circles depict phosphoproteins interrogated by phosphoproteomic analysis. Dashed lines indicate that the signaling intermediates between the two nodes have not been characterized in detail. (E) Dose-response analysis of Met autophosphorylation in GTL16 cells treated with increasing concentrations of PHA for 2 hours. (F) Heat map of phosphoprotein response to PHA-mediated Met inhibition in GTL16 cells. The color scale bar represents relative protein phosphorylation changes calculated as log2(inhibited/noninhibited) of the mean of two technical replicates. Molecules in italic were interrogated with MesoScale, the others with Luminex.

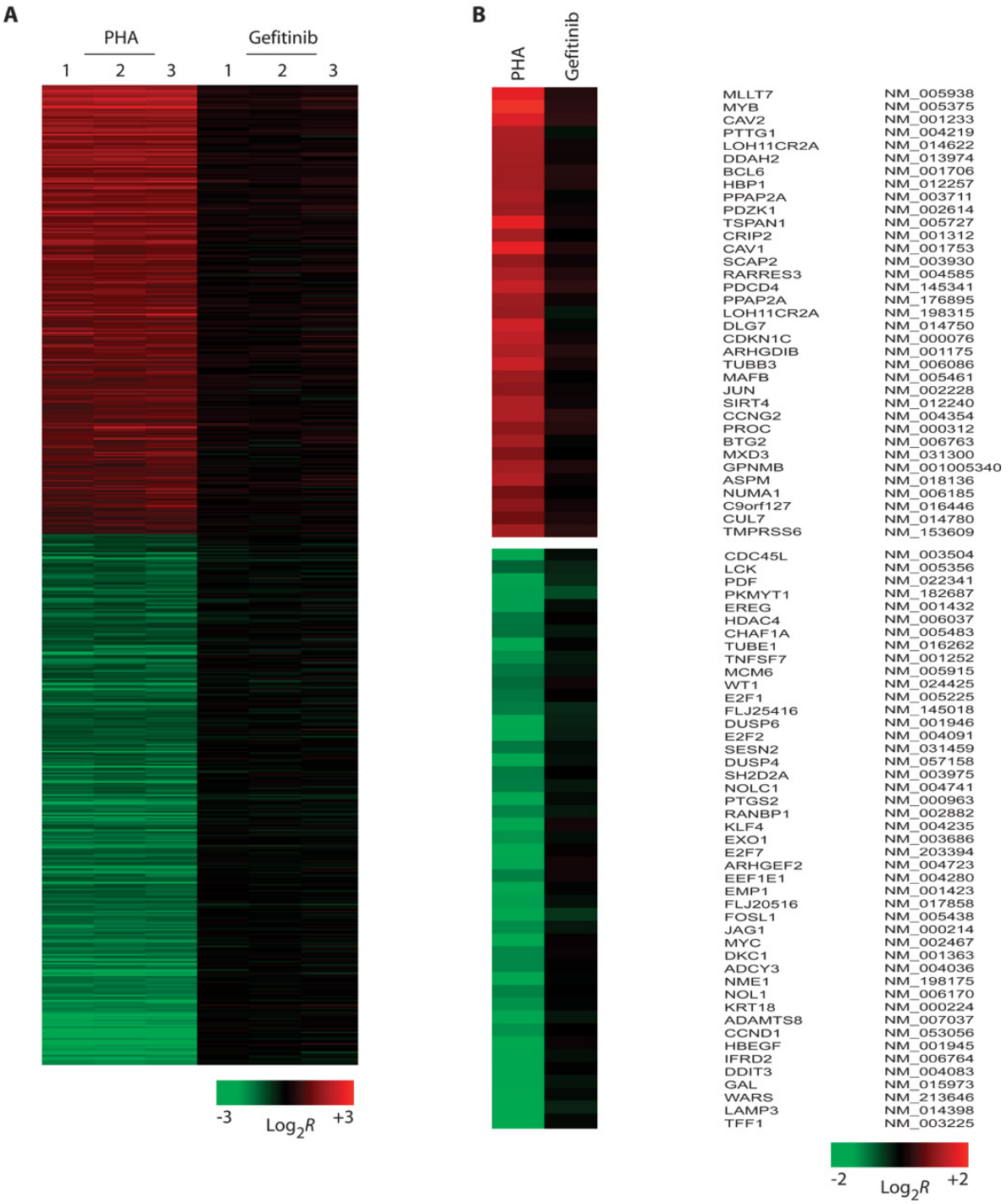

Figure 2. Met inhibition modulates the expression of genes in the Ras and PI3K pathways. (A) Heat map of gene expression signatures in response to PHA-mediated Met inhibition in GTL16 cells (three replicates). Expression profiles are not significantly affected by gefitinib. The color scale bar represents relative gene expression changes calculated as log2(inhibited/noninhibited). (B) List and expression changes of cell-cycle genes (according to GO annotations) modulated by Met inhibition.

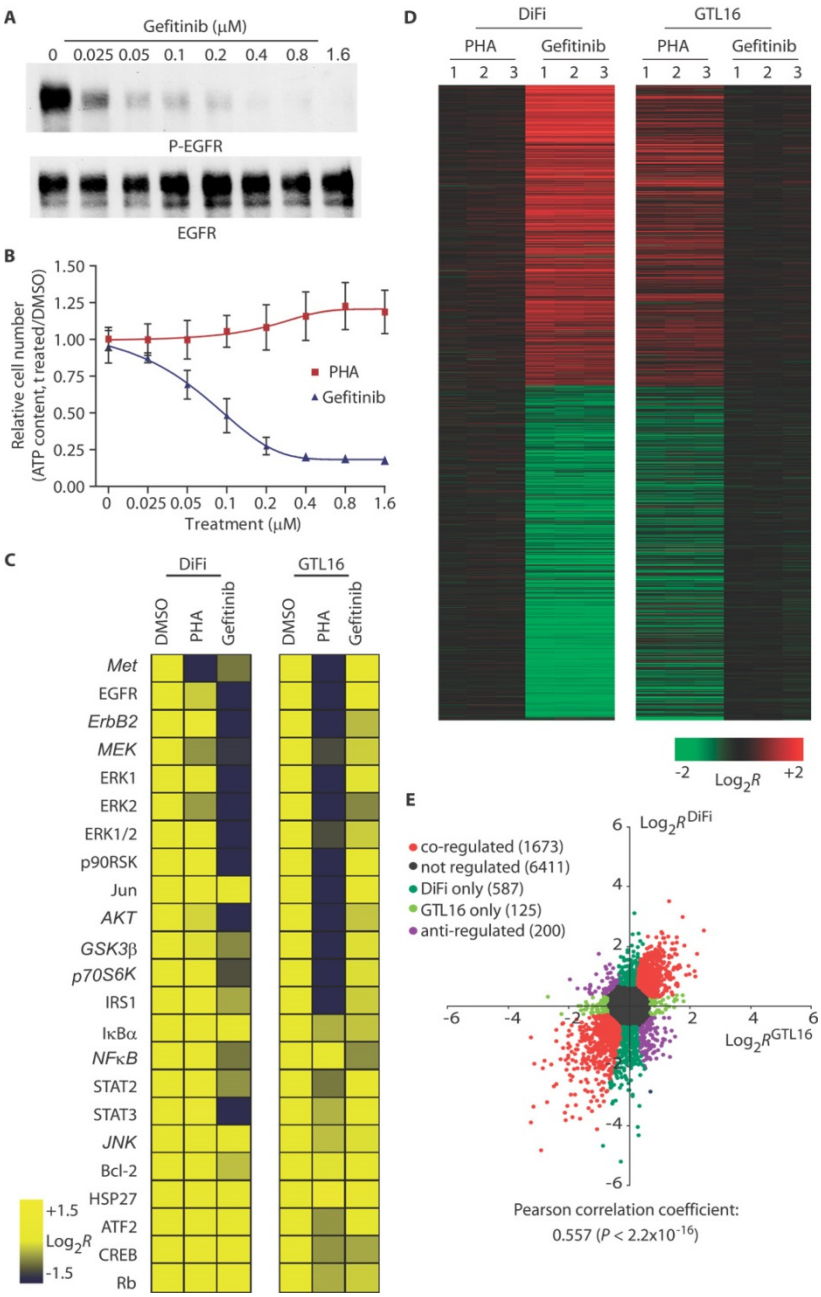

Figure 3. Common response signatures for Met and EGFR inhibition. (A) Dose-response analysis of EGFR autophosphorylation in DiFi cells treated with increasing concentrations of gefitinib for 2 hours. (B) Inhibition of proliferation in DiFi cells treated for 96 hours with increasing concentrations of gefitinib. PHA is ineffective. Data are the means ± SD of eight samples (two independent experiments performed in quadruplicate). (C) Heat map of phosphoprotein response to gefitinib-mediated EGFR inhibition in DiFi cells. The heat map of GTL16 is the same as in Fig. 1F and is shown for comparison. (D) Heat map of gene expression signatures in response to EGFR inhibition in DiFi (three replicates). The heat map of GTL16 is the same as in Fig. 2A and is shown for comparison. (E) Two-sample correlation plot of gefitinib-treated DiFi and PHA-treated GTL16. Analysis covers all the transcripts expressed by both cell lines, and co-regulated changes have been filtered using low-stringency criteria for gene inclusion ([log2RGTL16 + log2RDiFi]2 > 1, 0.3 < log2RGTL16/log2RDiFi < 3). The Pearson product-moment coefficient, reflecting the degree of linear relationship between two variables, was calculated as a measure of co-regulation of the data sets; P value represents the probability that the correlation coefficient is 0 (null hypothesis).

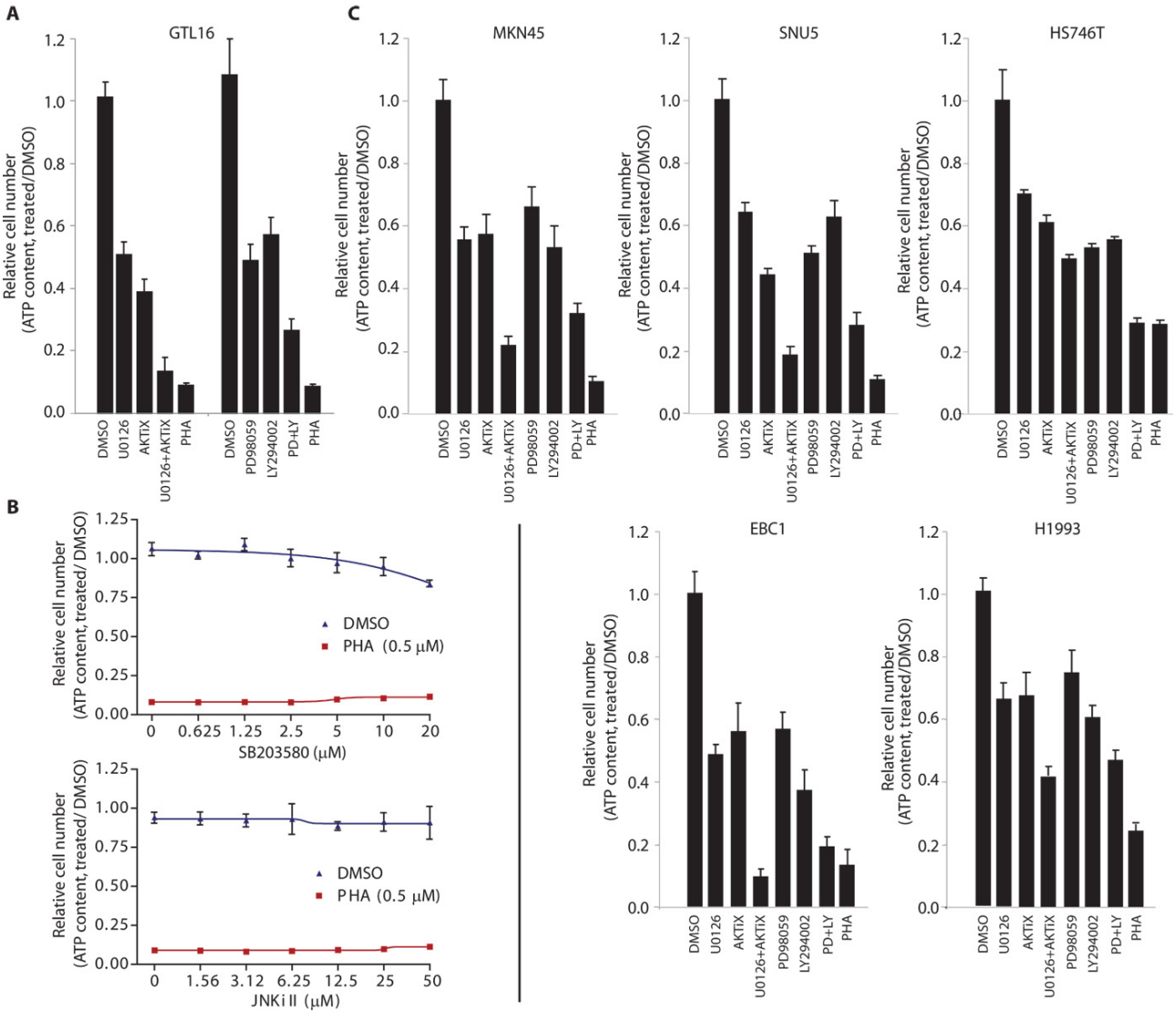

Figure 4. MEK, PI3K, and AKT inhibition, but not p38 or JNK inhibition, impairs proliferation of Met-addicted cell lines. (A) Inhibition of proliferation of GTL16 cells treated with the indicated inhibitors for 96 hours. The inhibitors were used at 10 μM concentration except for PD98059, which was used at 30 μM. PHA was used at 0.5 μM. (B) Dose-response proliferation (viability) assay in GTL16 cells treated with increasing concentrations of the p38 inhibitor SB203580 or the JNK inhibitor II (JNKi II), in the absence (blue) or presence (red) of 0.5 μM PHA for 96 hours. Pharmacologic inhibition of p38 or JNK does not affect cell proliferation per se nor sensitivity to PHA. (C) Inhibition of proliferation of MKN45, SNU5, HS746T, EBC1, and H1993 cells treated with the indicated inhibitors for 96 hours. The inhibitors were used at the same concentrations as in (A). All data are the means ± SD of eight samples (two independent experiments performed in quadruplicate).

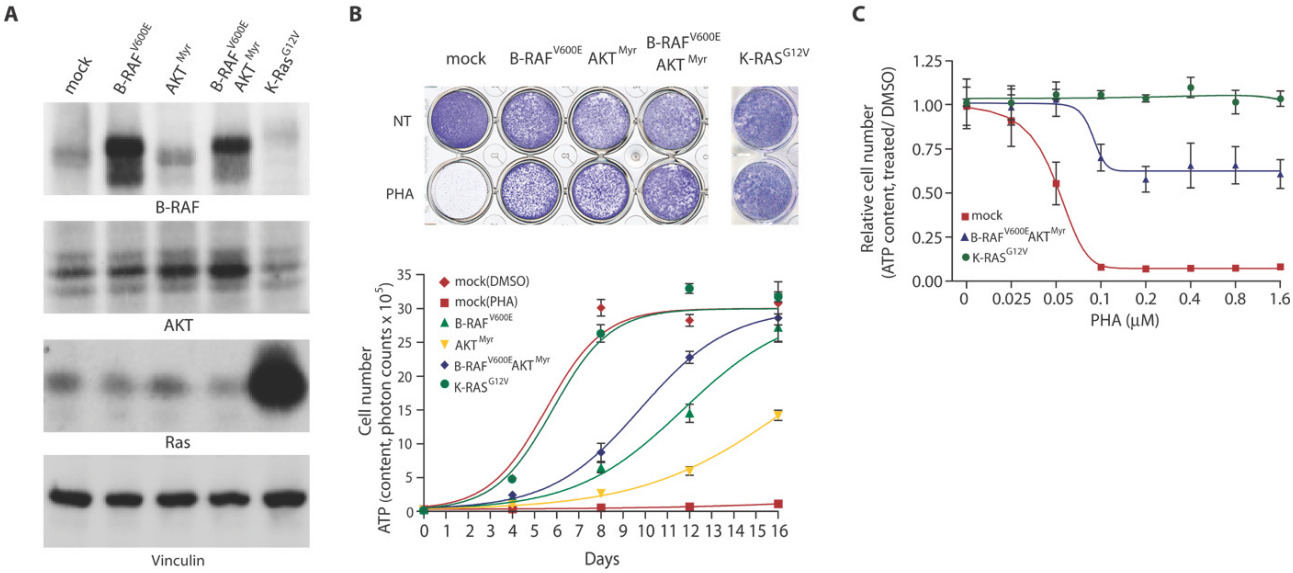

Figure 5. Active mutants of Ras, RAF, or AKT induce biological resistance to Met inhibition. (A) Western blots showing the abundance of the exogenously introduced B-RAFV600E, AKTMyr, or RasG12V in GTL16 cells. (B) GLT16 cells infected with the indicated constructs were either left untreated (NT) or incubated with 0.5 μM PHA for 16 days, after which cells were fixed, stained, and photographed (upper panel). Cell proliferation during this incubation period was also monitored quantitatively every 4 days (lower panel). Data are the means ± SD of eight samples (two independent experiments performed in quadruplicate). Basal growth curves (in the absence of PHA) are reported in fig. S6. (C) Inhibition of proliferation in control GTL16 cells (mock), cells coexpressing B-RAFV600E and AKTMyr, and cells expressing RasG12V. Cells were treated for 96 hours with increasing concentrations of PHA. Data are the means ± SD of eight samples (two independent experiments performed in quadruplicate).

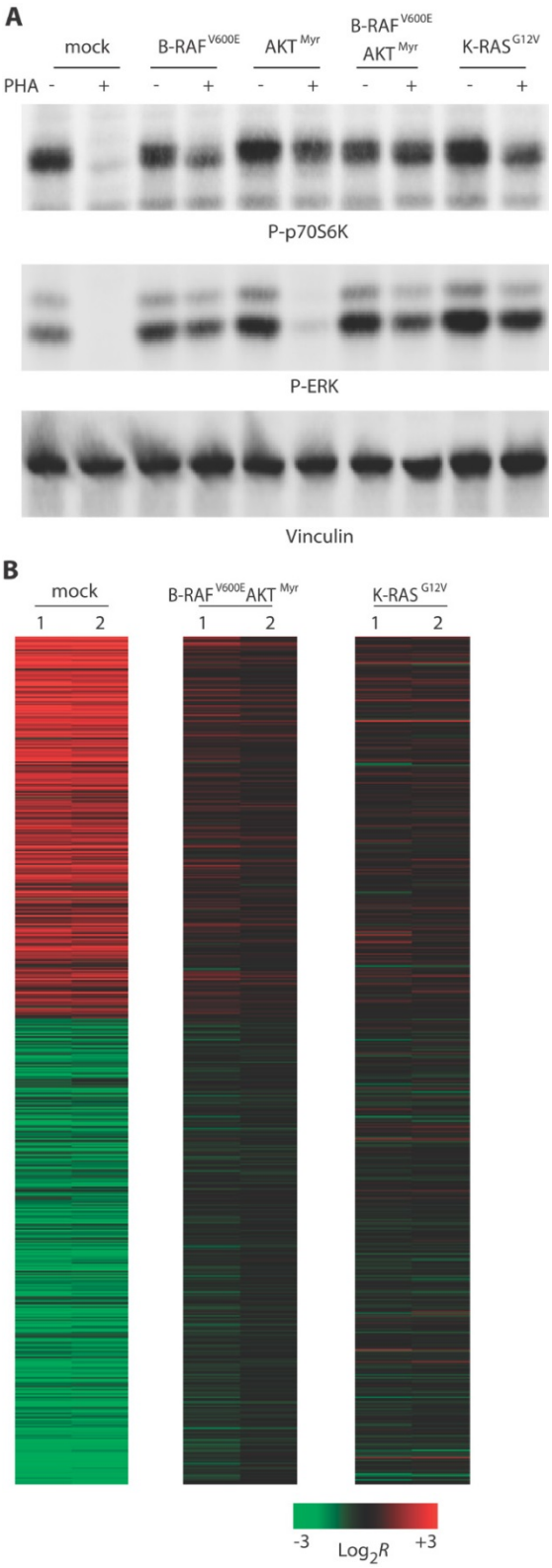

Figure 6. Active mutants of Ras, RAF, and AKT induce biochemical and transcriptional resistance to Met inhibition. (A) Phosphorylation of p70S6K and ERK1/2 in GTL16 cells expressing the indicated constructs, in the presence or absence of 1 μM PHA for 2 hours. The Western blot is representative of four experiments. (B) Heat map of gene expression signatures in response to Met inhibition in control GTL16 (mock); GTL16 coexpressing B-RAFV600E and AKTMyr; and GTL16 expressing RasG12V (two replicates).

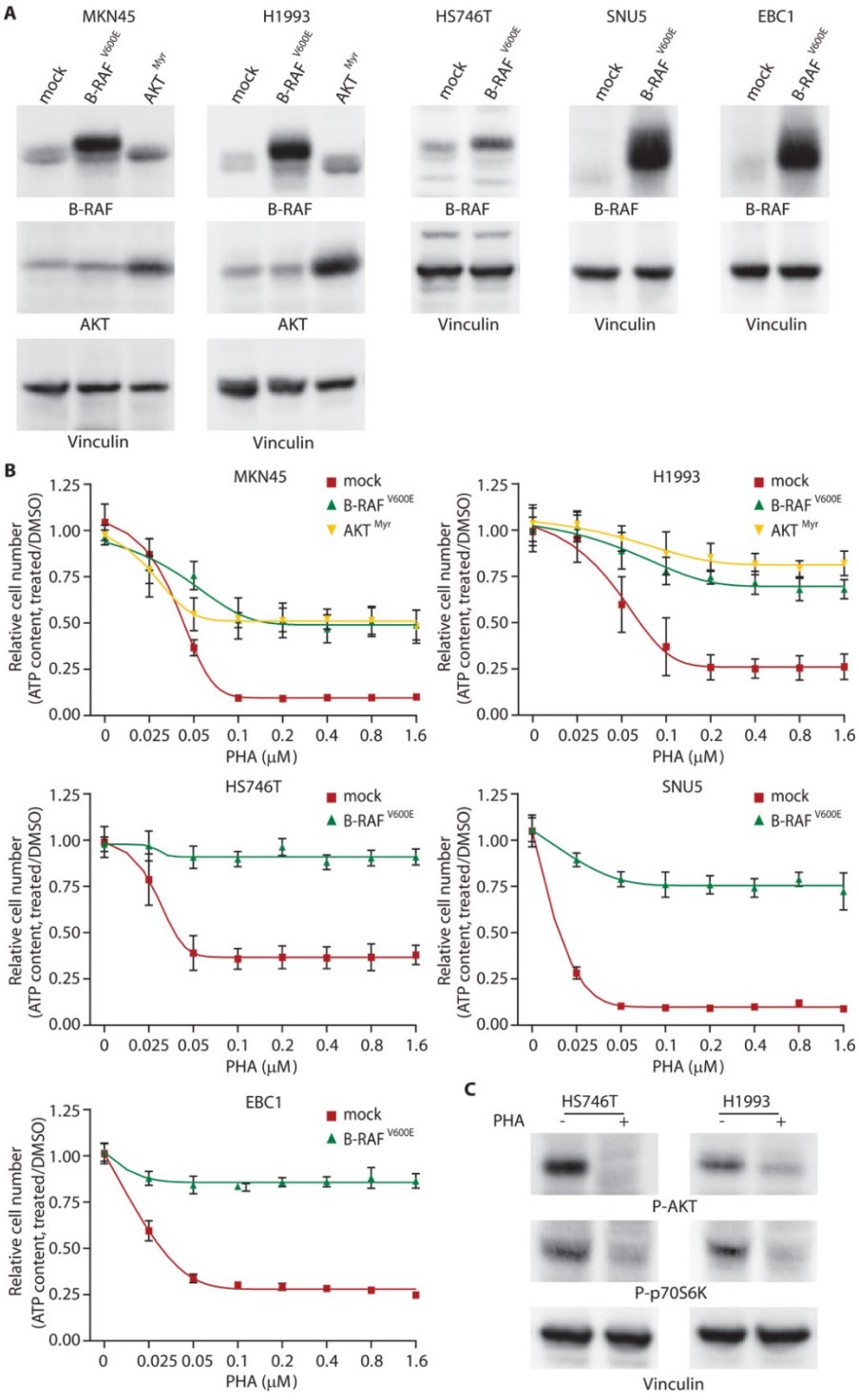

Figure 7. Active mutants of RAF and AKT induce resistance to Met inhibition in various Met-addicted cell lines. (A) Western blots showing the abundance of exogenously introduced B-RAFV600E and AKTMyr in the indicated cell lines. (B) Inhibition of proliferation in control cells (mock) and in cells expressing B-RAFV600E or AKTMyr, treated for 96 hours with increasing concentrations of PHA. Data are the means ± SD of eight samples (two independent experiments performed in quadruplicate. (C) The E545A PIK3CA mutation does not prevent Met-dependent modulation of downstream effectors. HS746T and H1993 cells, both displaying the E545A mutation of the PIK3CA gene, were treated with 0.5 μM PHA for 2 hours. Met inhibition results in reduced phosphorylation of the PI3K effectors AKT and p70S6K.

Table 1. GSEA analysis of the transcriptional response produced by Met pharmacologic inhibition in GTL16 cells. The gene sets, all statistically significant, have been selected on the basis of their functional importance and are ranked by normalized enrichment score (NES). ES, enrichment score; NOM, nominal; FDR, false discovery rate.

Rank	Gene set	Size	ES	NES	NOM *P* value	FDR *q* value
Up						
2	SERUM_FIBROBLAST_CORE_DN	187	0.48	2.2	<0.001	0.001
11	PENG_RAPAMYCIN_UP	161	0.44	1.96	<0.001	0.012
20	CORDERO_KRAS_KD_VS_CONTROL_UP	77	0.47	1.88	<0.001	0.02
Down						
1	SCHUMACHER_MYC_UP	53	−0.81	−2.98	<0.001	<0.001
2	PENG_RAPAMYCIN_DN	192	−0.63	−2.85	<0.001	<0.001
7	SERUM_FIBROBLAST_CORE_UP	189	−0.56	−2.55	<0.001	<0.001
17	REN_E2F1_TARGETS	40	−0.66	−2.29	<0.001	<0.001
20	CORDERO_KRAS_KD_VS_CONTROL_DN	56	−0.60	−2.21	<0.001	<0.001

Table 2. GSEA analysis of co-regulated transcripts after EGFR inhibition in DiFi cells and Met inhibition in GTL16 cells. The gene sets have been selected based on the list presented in Table 1 and are ranked by normalized enrichment score (NES). ES, enrichment score; NOM, nominal; FDR, false discovery rate.

Rank	Gene set	Size	ES	NES	NOM *P*value	FDR *q*value
Up						
3	SERUM_FIBROBLAST_CORE_DN	48	0.44	2.24	<0.001	0.003
5	PENG_RAPAMYCIN_UP	28	0.47	2.06	<0.001	0.012
Down						
1	PENG_RAPAMYCIN_DN	50	−0.65	−3.04	<0.001	<0.001
4	SERUM_FIBROBLAST_CORE_UP	52	−0.61	−2.90	<0.001	<0.001
8	SCHUMACHER_MYC_UP	29	−0.67	−2.69	<0.001	<0.001

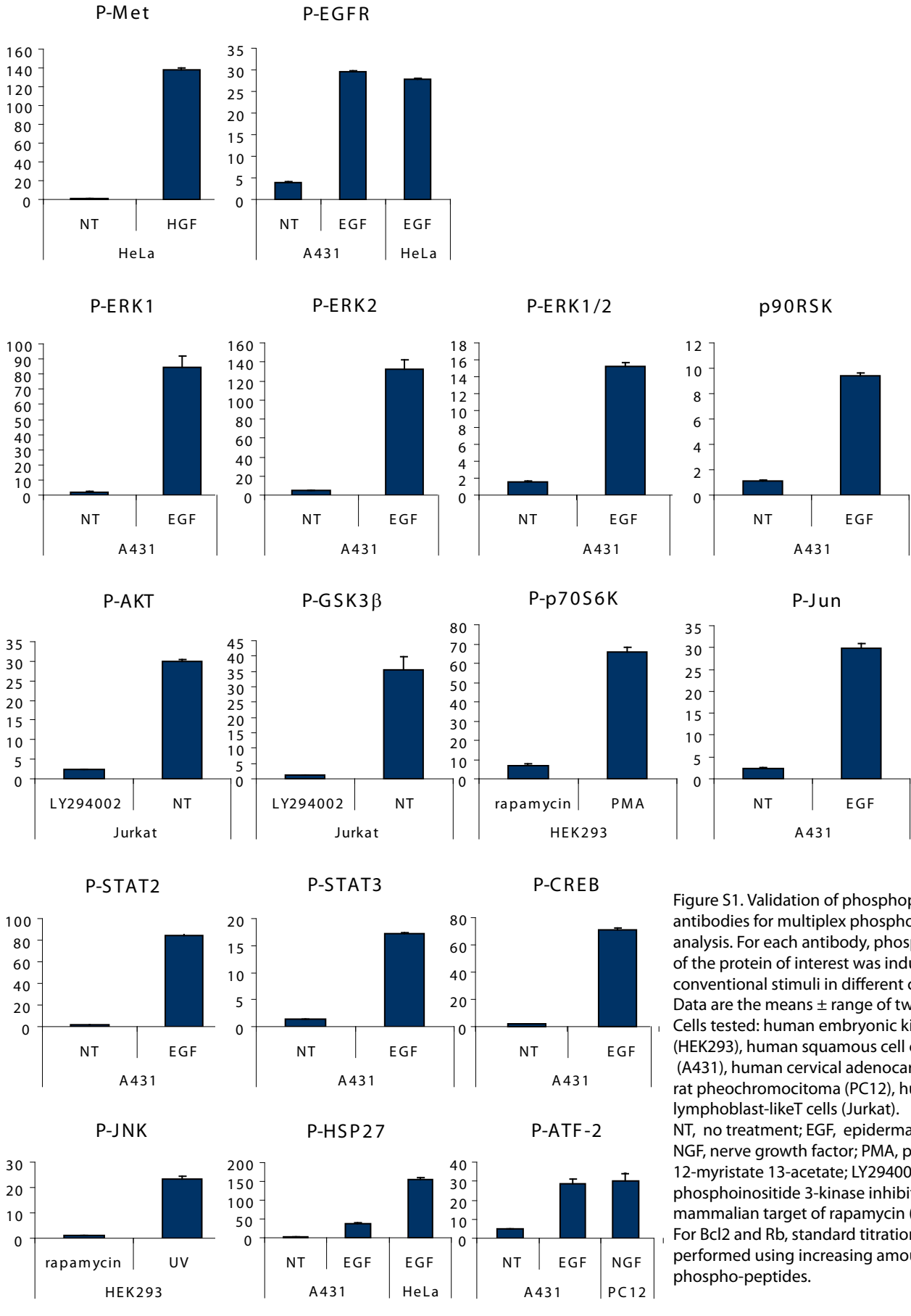

Figure S1. Validation of phosphoprotein antibodies for multiplex phosphoproteomics analysis. For each antibody, phosphorylation of the protein of interest was induced by conventional stimuli in different cell lines. Data are the means ± range of two replicates. Cells tested: human embryonic kidney (HEK293), human squamous cell carcinoma (A431), human cervical adenocarcinoma (HeLa), rat pheochromocitoma (PC12), human lymphoblast-likeT cells (Jurkat).
NT, no treatment; EGF, epidermal growth factor; NGF, nerve growth factor; PMA, phorbol 12-myristate 13-acetate; LY294002, phosphoinositide 3-kinase inhibitor; rapamycin, mammalian target of rapamycin (mTOR) inhibitor. For Bcl2 and Rb, standard titration curves were performed using increasing amounts of purified phospho-peptides.

Bertotti et al., Figure S1

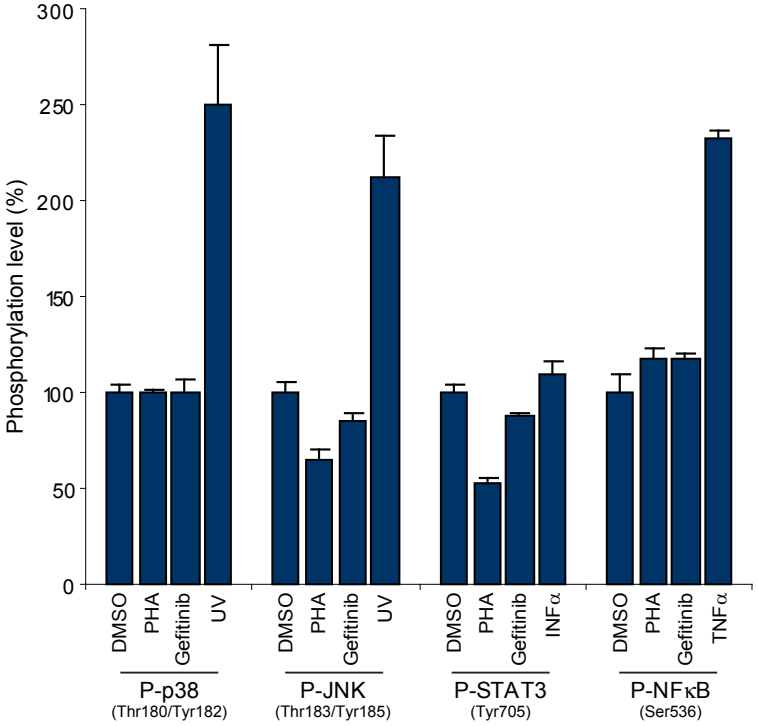

Figure S2. Met inhibition has little or no effects on the activation of p38 MAPK, JNK, STAT3, and NF-κB.
The relative phosphorylation of p38 MAPK, JNK, STAT3, and NF-κB in GTL16 cells treated for 2 h with 0.4 μM PHA, as assessed by ELISA. Treatment with 0.4 μM gefitinib for 2 h was used as a negative control. Positive controls were the following: UV irradiation (1.2 J/m^2, 20 s) for p38 MAPK and JNK; interferon-alpha (IFN-α) (100 ng/ml, 10 min) for STAT3; tumor necrosis factor-alpha (TNF-α) (10 ng/ml, 10 min) for NF-κB. Data are the means ± SD of six samples (two independent experiments performed in triplicate).

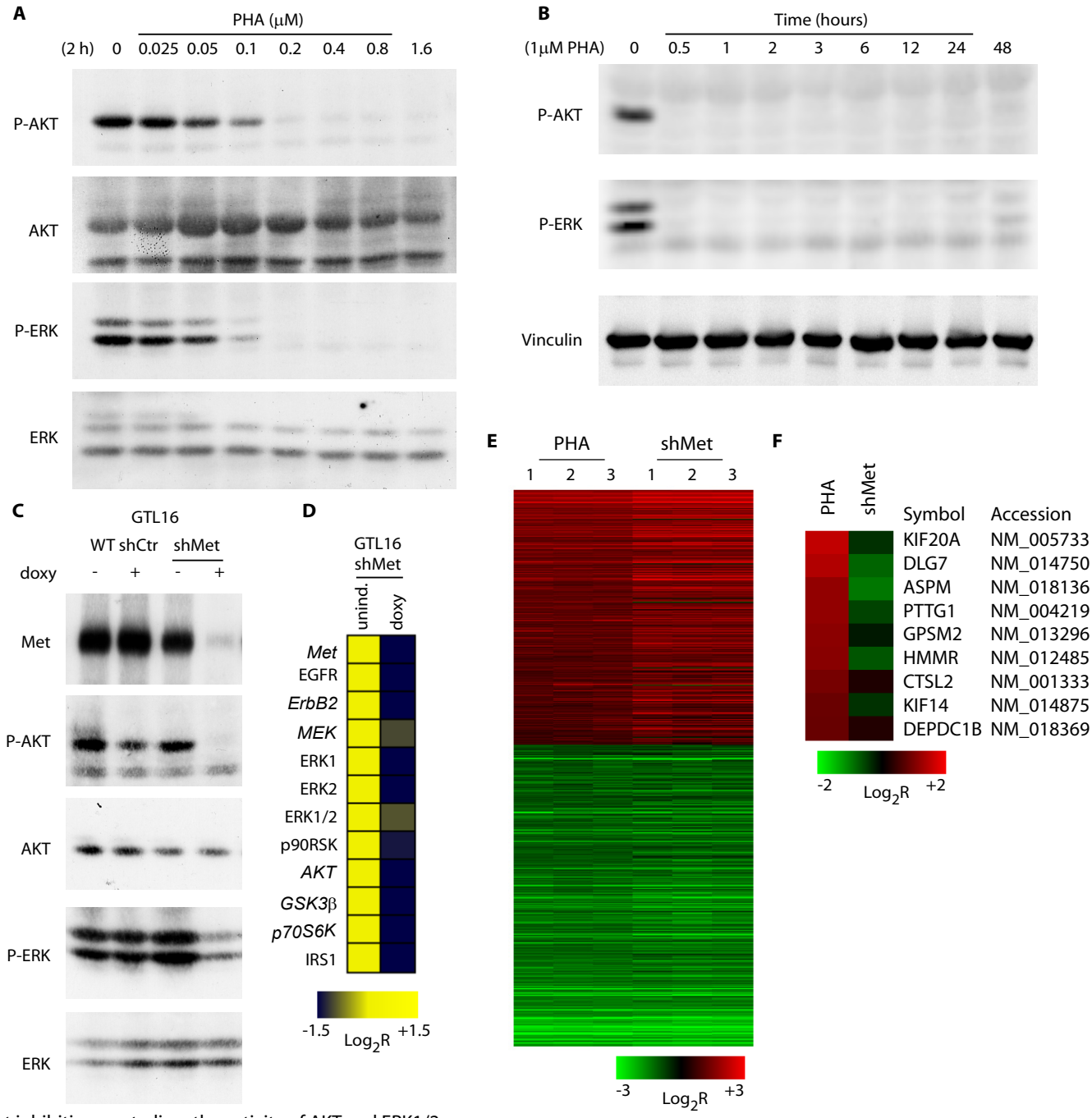

Figure S3. Met inhibition neutralizes the activity of AKT and ERK1/2.
(A) Dose-response analysis of AKT and ERK1/2 phosphorylation in GTL16 cells treated with increasing concentrations of PHA for 2 h. (B) Time-course analysis of AKT and ERK1/2 phosphorylation in GTL16 treated with 1 μM PHA. (C) Inhibition of AKT and ERK1/2 phosphorylation by doxycycline-inducible knockdown of Met. The abundance of Met and the amount of phosphorylation of AKT and ERK1/2 in wild-type GTL16 (WT); GTL16 infected with a non-targeting small hairpin RNA (shCtr) and treated with doxycyclin (+); GTL16 infected with a Met-targeting shRNA (shMet) and either left untreated (-) or treated with doxycycline (+). (D) Heat map of selected phosphoprotein responses to RNAi-mediated inactivation of Met in GTL16 cells.
(E) Comparative heat map of gene expression signatures in GTL16 following treatment with 1 μM PHA or RNAi-mediated, doxycycline-induced knockdown of Met. The heat map of PHA-treated GTL16 is the same as in Figure 2A and is shown for comparison. (F) List and expression changes of the genes that are discordantly modulated by PHA treatment versus shRNA induction in GTL16 cells.

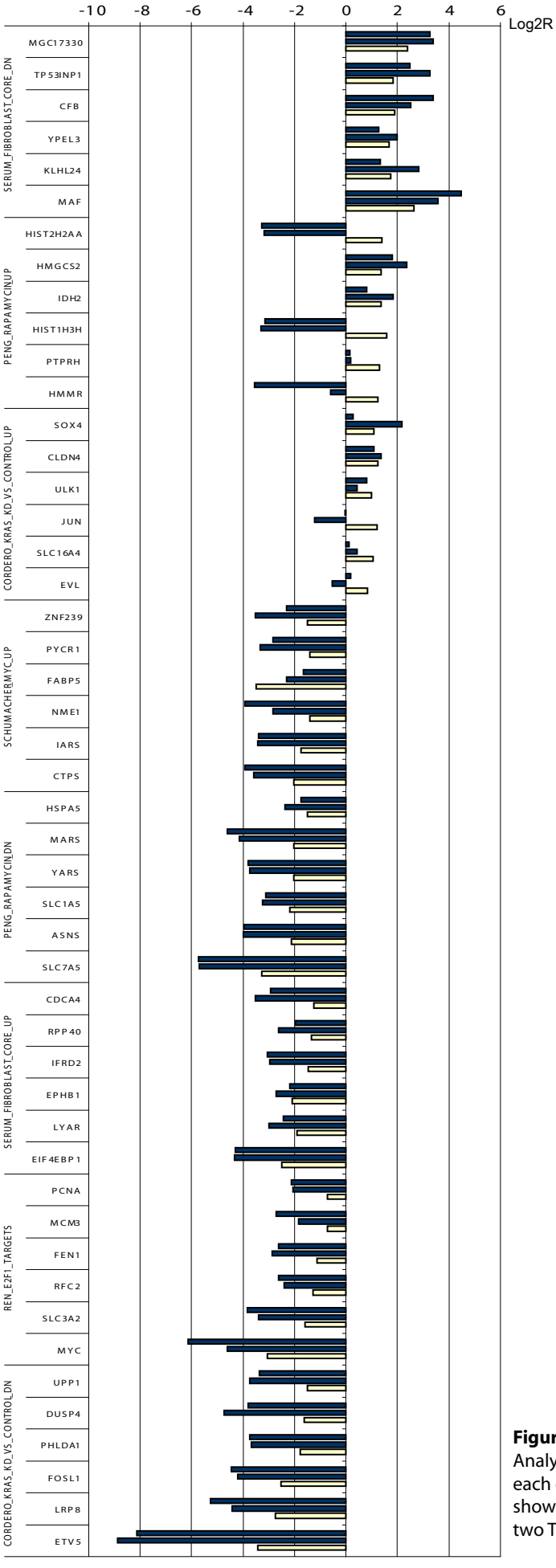

Figure S4. Microarray validation by TaqMan low-density quantitative PCR arrays. Analysis was performed on the six genes with highest enrichment score for each of the the eight gene sets listed in Table 1. For each gene, histograms show the mean value of microarray triplicates (yellow bar) and the values of the two TaqMan replicates (blue bars) for comparison.

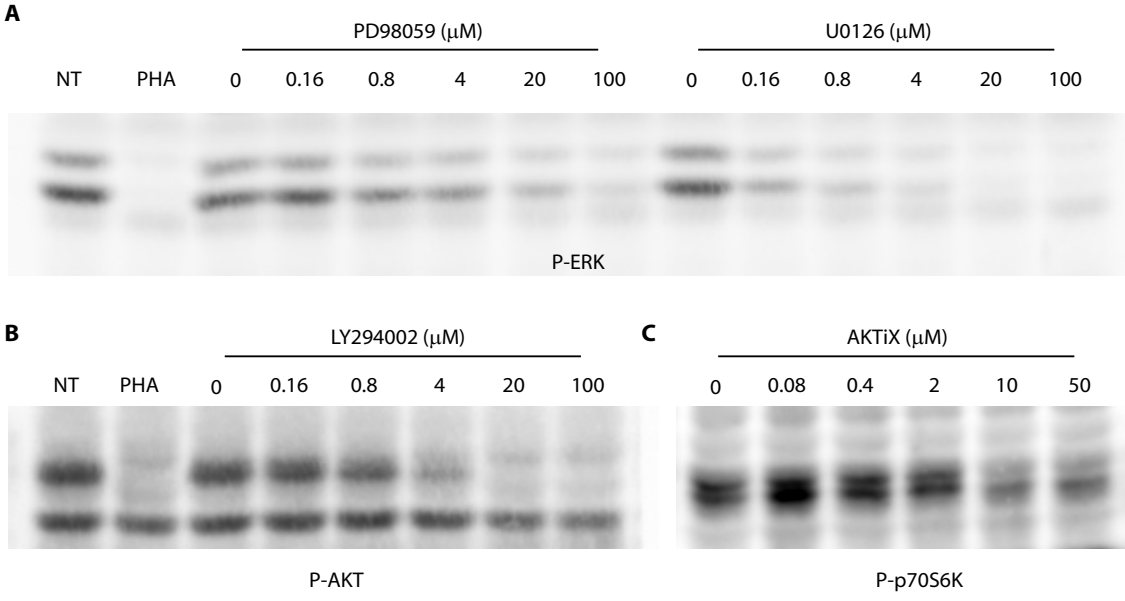

Figure S5. Effects of MEK, PI3K, and AKT inhibitors on downstream effectors in GTL16 cells.
(A) GTL16 cells were treated for 2 h with increasing concentrations of the MEK inhibitors PD98059 or U0126. Both compounds dose-dependently inhibit ERK1/2 phosphorylation. Inhibition of ERK1/2 phosphorylation by PHA is shown as a control.
(B) GTL16 cells were treated with increasing concentrations of the PI3K inhibitor LY294002. Phosphorylation of AKT decreases in a dose-dependent manner. Inhibition of AKT phosphorylation by PHA is shown as a control.
(C) GTL16 cells were treated with increasing concentrations of the AKT inhibitor X (AKTiX). Phosphorylation of p70S6K decreases in a dose-dependent manner.

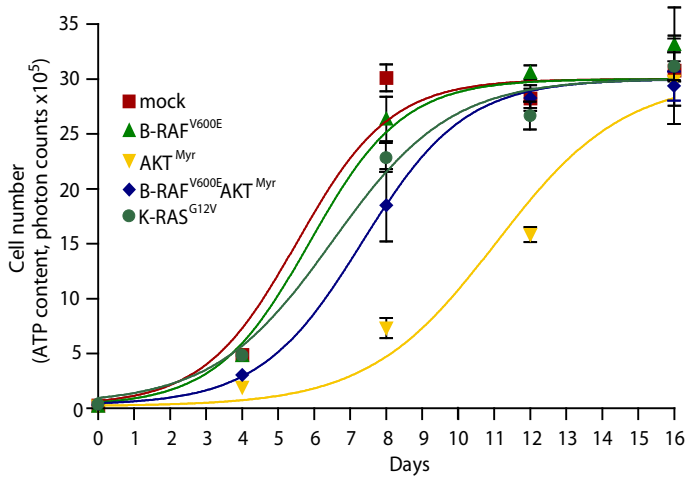

Figure S6. Basal proliferation curves of PHA-resistant GTL16 cells.
Proliferation of GLT16 cells infected with the indicated constructs in the absence of PHA, monitored quantitatively every four days. Data are the means ± SD of eight samples (two independent experiments performed in quadruplicate).